

**CONVERGENCE ANALYSIS OF AN ADAPTIVE
INTERIOR PENALTY DISCONTINUOUS GALERKIN
METHOD FOR THE HELMHOLTZ EQUATION**

A Dissertation

Presented to

the Faculty of the Department of Mathematics

University of Houston

In Partial Fulfillment

of the Requirements for the Degree

Doctor of Philosophy

By

Natasha S. Sharma

December 2011

CONVERGENCE ANALYSIS OF AN ADAPTIVE
INTERIOR PENALTY DISCONTINUOUS GALERKIN
METHOD FOR THE HELMHOLTZ EQUATION

Natasha S. Sharma

APPROVED:

Prof. Ronald H. W. Hoppe.

Prof. Roland Glowinski

Prof. Yuri Kuznetsov

Prof. Tim Warburton

Dean, College of Natural Sciences and Mathematics

Acknowledgements

It would be very unfair if I did not begin this note of acknowledgement without mentioning the contribution of the mathematician Frigyes Riesz -Reisz lemma. An application of this lemma in the guaranteeing a weak solution to the variational formulation gave me enough reason to devote my Ph.D years to investigate the interplay of functional analysis and partial differential equations .

A special thanks to Dr Tim Warburton for carefully proof reading my thesis, providing useful feedback, and for posing interesting questions. I would also like to thank Dr Warburton for introducing me to the nudg library and going beyond that by patiently walking through my computing issues during my initial years of Ph.D. All my seniors in the Math Department of UH have been a source of inspiration in particular Dr Harbir Antil, Dr Oleg Boiarkine, Dr T.W. Pan, and Dr Aarti Jajoo. Leading by example their hard work and dedication to science is a silent testament of the level of perseverance that one can only be in awe of.

I would like to extend a special thanks to Dr Giles Auchmuty and Dr Yuri Kuznetsov for entertaining my naive questions and discussions, and Dr Glowinski for his cheery nature and encouraging conversations. I would also like to acknowledge the financial support provided by National Science Foundation in the past three years.

One person who made everything fall into the right place is my advisor-Dr Hoppe for bringing together all these influences in my academic career as well as providing an excellent introduction to numerical methods to partial differential equation. Dr Hoppe, I cannot overemphasize your role in making all this possible. Thank you for

choosing me for this project.

During my early years in India, I would to thank Dr Dinesh Singh, Dr Sanjeev Agrawal, my colleague and friend Pankaj for challenging my curious mind, Dr Amber Habib for being an excellent teacher, and Dr Pradeep Narain for introducing me to real analysis in my early undergraduate years.

On a personal level, this thesis is purely dedicated to all those who constitute the wind beneath my wings - my parents, Anjali, Radhika, Shyams, Megha, Anando, Ankita, Aanchal and Flora.

Last but not the least, I would to acknowledge the support of Dr. Annalisa Quaini for always having that welcoming chair ready for me in her office and for helping me realize the three core pursuits in our life - adventure, culture, nature.



To Womsilet Shilla and K.P Sharma

**CONVERGENCE ANALYSIS OF AN ADAPTIVE
INTERIOR PENALTY DISCONTINUOUS GALERKIN
METHOD FOR THE HELMHOLTZ EQUATION**

An Abstract of a Dissertation
Presented to
the Faculty of the Department of Mathematics
University of Houston

In Partial Fulfillment
of the Requirements for the Degree
Doctor of Philosophy

By
Natasha S. Sharma
December 2011

Abstract

In this thesis, we are mainly concerned with the numerical solution of the two dimensional Helmholtz equation by an adaptive Interior Penalty Discontinuous Galerkin (IPDG) method based on adaptively refined simplicial triangulations of the computational domain. The a posteriori error analysis involves a residual type error estimator consisting of element and edge residuals and a consistency error which, however, can be controlled by the estimator. The refinement is taken care of by the standard bulk criterion (Dörfler marking) known from the convergence analysis of adaptive finite element methods for linear second-order elliptic PDEs. The main result is a contraction property for a weighted sum of the energy norm of the error and the estimator which yields convergence of the adaptive IPDG approach. Numerical results are given that illustrate the quasi-optimality of the method.

Contents

1	Introduction	2
2	Adaptive Cycle	6
2.1	SOLVE	7
2.2	ESTIMATE	8
2.3	MARK	9
2.4	REFINE	9
3	Convergence Analysis	11

3.1	Screen Problem	13
3.2	The IPDG Method	14
3.3	A Posteriori Error Analysis	21
	3.3.1 Reliability	28
	3.3.2 Efficiency	30
3.4	Quasi-orthogonality	35
	3.4.1 Mesh Perturbation Result	36
	3.4.2 Lower order Term	37
	3.4.3 Quasi-orthogonality	39
3.5	Contraction Property	44
4	Numerical Results	47
4.1	Introduction	47
4.2	Preliminary Results for Smooth Problems	48
4.3	Test Problems on Non-convex Domain	49
	4.3.1 L-shaped Domain	51
	4.3.2 Pacman Problem	52
	4.3.3 Screen Problem	53

4.4 Convex Domain	57
6 Conclusions and Future Work	60
Bibliography	62

List of Figures

2.1	Newest vertex bisection: Assign one of the vertices as the new vertex a_2 , refinement is done by connecting a_2 to the midpoint a^* of the edge connecting a_1 and a_3	10
4.1	A comparison of the convergence for different polynomial order N for wave numbers $k = 5$ (left), $k = 10$ (center) and $k = 20$ (right)	49
4.2	Exact solution for $k = 20$ (left) and adaptively refined grid after 8 refinement steps for $k = 10$, $N = 6$, and $\theta = 0.3$ (right).	51
4.3	Convergence history of the adaptive IPDG method. Mesh dependent energy error as a function of the DOF (degrees of freedom) on a logarithmic scale: $k = 5$, $N = 6$ (left) and $k = 10$, $N = 6$ (left).	52

4.4	Adaptively refined grids for $k = 1$, $N = 4$, $\theta = 0.1$ (left) and $k = 5$, $N = 6$, $\theta = 0.3$ (right) after 6 and 3 levels of the adaptive cycle	53
4.5	Convergence history of the adaptive IPDG method. Mesh dependent energy error as a function of the DOF (degrees of freedom) on a logarithmic scale: $k = 5$, $N = 4$ (left) and $k = 5$, $N = 6$ (left).	54
4.6	Real part of the computed IPDG approximation for $k = 15$ (left) and $k = 20$ (right).	54
4.7	Adaptively refined mesh for $k = 10$, $N = 6$ after 8 refinement steps (left) and for $k = 20$, $N = 6$ after 12 refinement steps (right).	55
4.8	Convergence history of the adaptive IPDG method. Error estimator as a function of the DOF (degrees of freedom) on a logarithmic scale: $k = 10$, $N = 4$ (left) and $k = 10$, $N = 6$ (right).	55
4.9	Convergence history of the adaptive IPDG method. Error estimator as a function of the DOF (degrees of freedom) on a logarithmic scale: $k = 15$, $N = 4$ (left) and $k = 15$, $N = 6$ (left).	56
4.10	Computed solution (left) and exact solution (right) for $k = 70$	57
4.11	h -convergence using linear elements (left);quadratic elements (right).	58
4.12	Convergence of the discretization error $\ u - u_h\ _{0,\Omega}$ as a function of the DOF (degrees of freedom) on a logarithmic scale: $k = 70$, $N = 4$ (left) and $k = 70$, $N = 6$ (left).	59

4.13 Convergence history of the adaptive IPDG method. Mesh dependent energy error as a function of the DOF (degrees of freedom) on a logarithmic scale: $k = 70$, $N = 4$ (left) and $k = 70$, $N = 6$ (left). 59

CHAPTER 1

Introduction

An a posteriori error analysis for the acoustic wave propagation problems is of practical significance to physicists and engineers particularly for providing reliable upper bounds on the error that arises due to the fact that the exact solution is approximated by a discrete solution which is computed on a mesh consisting of grid points. The phenomena of acoustic wave propagation is characterized by the following Helmholtz equation:

$$\frac{\partial^2 u}{c^2 \partial t^2} = \Delta u$$

The solution of this equation, whether achieved directly in the time domain or whether limited to periodic frequency domain, always results in wave phenomena.

Our convergence analysis is concerned with solutions in the frequency domain and mathematically assume the form:

$$-\Delta u - \kappa^2 u = f \tag{*}$$

where κ denotes the wavenumber and the quality of the numerical solution depends significantly on it. One of the main challenges is in the accurate resolution of highly oscillatory solutions to the Helmholtz equation for large wavenumber and an intuitive idea to improve the accuracy is to consider a meshsize h which is small enough to include the same number of grid points per wavelength.

It is known that for grids satisfying the mesh constraint $\kappa h \lesssim 1$, the errors of the finite element solution deteriorate as κ increases [8]. This non-robust behavior in relation to κ is known as the pollution effect [8, 36]. Pioneering work was initiated by Babuška and his collaborators to carefully analyze the pollution effect [8] in particular a finite element error analysis in [11] revealed that the relative error e_1 of the finite element solution with respect to the H^1 -semi norm is bounded above by the sum of error in the best approximation C_1 and a second term C_2 which is associated with the pollution effect as shown below:

$$e_1 \leq \psi C_1 + \kappa \psi^2 C_2 \quad \text{where } \psi = \left(\frac{\kappa h}{2N}\right)^N.$$

This sum is scaled by a factor ψ and so evidently for high wavenumber κ , this pollution error C_2 dominates the upper bound and thus leads to the non-robust behavior with respect to the wavenumber.

Intuitively, one can circumvent this difficulty by either decreasing the mesh size h or increasing the polynomial order N both these approaches are constrained to the

limited computational resources at our disposal.

Furthermore, the presence of singularities arising in the problems necessitates the introduction of an optimal adaptive mesh refinement. In this thesis, we propose an adaptive Interior Penalty Discontinuous Galerkin (IPDG) Method using higher order elements for resolving the Helmholtz equation with high wavenumber in two dimensions. Our adaptive cycle depends on a residual-type error estimator that we will introduce in chapter 3. Therein, we establish its reliability and efficiency.

This thesis is organized as follows: the second chapter gives a brief outline of the adaptive algorithm with an emphasis on the marking and refinement step of the adaptive cycle.

The heart of the thesis lies in the third chapter which we begin with a brief description of the screen problem and introduce its IPDG approximation with respect to a shape regular family of simplicial triangulations. The adaptive mesh refinement is based on a residual-type a posteriori error estimator which is shown to control the energy norm of the discretization error as well as the consistency error that arises due to the non-conformity of the Galerkin method.

Our convergence analysis involves establishing the reliability of the estimator, a reduction property for this estimator as well as a quasi-orthogonality result. As in the convergence analysis for standard second-order elliptic problems (cf. [15, 41, 34]) establishing these three properties is crucial for proving a contraction property. However, the presence of a lower order term in the Helmholtz equation (*) demands a special treatment and to this end, we follow the approach as suggested in [29]. This idea involves resorting to the conforming approximation of the Helmholtz equation

and employing an Aubin-Nitsche's type duality argument. Finally, we prove the contraction property which guarantees the convergence of the method.

The fourth chapter provides numerical validation for the proposed method based on a range of test problems. In particular, we focus on the screen problem for which the analytic solution is unknown.

Finally, our last chapter concludes this thesis with some possible future directions including extending the analysis to three-dimensional time harmonic Maxwell's equations.

CHAPTER 2

Adaptive Cycle

The subject of error estimation and adaptive refinement necessary to achieve a specified accuracy was first introduced to the finite element field by Babuška and his collaborators [6],[7]. He was the first to show that reasonable error estimation could be achieved at a cost less than that of the original solution and he also defined the possible paths to refinement namely h -refinement, which required mesh subdivision, or p -refinement, where addition of higher order polynomial terms to the element form was used, and finally hp -refinement, where a little of each procedure was used.

Even though adaptive finite element method was a fundamental tool in improving the approximation of under resolved solutions, it is only recently in 1996 that Dörfler

[23] initiated the convergence analysis for standard second-order elliptic problems.

The adaptive algorithm consists of:

$$\text{SOLVE} \rightarrow \text{ESTIMATE} \rightarrow \text{MARK} \rightarrow \text{REFINE}$$

The aim of this algorithm is to iteratively improve the accuracy of the computed solution balancing this with the judicious use of number of unknowns and iterations involved.

The steps 'MARK' and 'REFINE' in the adaptive cycle are independent of the underlying variational problem. In this chapter, we briefly describe each of the steps.

2.1 SOLVE

We seek a discrete solution u_h in an appropriate finite element space V_h with respect to a triangulation $\mathcal{T}_h(\Omega)$ of the computational domain Ω such that

$$\mathcal{A}(u_h, v) = \ell(v), \quad v \in V_h, \quad \text{holds.}$$

Although it is a natural idea is to employ an iterative scheme to solving the complex symmetric, linear systems, this topic deserves a special investigation and in this thesis we rely on the accuracy of Matlab direct solver.

2.2 ESTIMATE

Based on the residual $r(v) := \mathcal{A}(u_h, v) - \ell(v)$, we obtain the error estimator η_h which consists of local element and edge residuals. These residuals are indicators which provide information about the regions in the domain where the numerical solution u_h is a poor approximation to the analytic solution u . Such an under resolution of the computed solution can be attributed to the presence of local singularities for instance, singularities which arise due to the presence of re-entrant corners.

Two desirable qualities we want η_h to possess are **reliability** and **efficiency**.

While an estimator is called **reliable** if it provides an upper bound for the error $u - u_h$ in the energy norm up to data oscillations osc_h^{rel} , that is we can find $C_{rel} > 0$, independent of mesh size h of $\mathcal{T}_h(\Omega)$ satisfying

$$\|u - u_h\|_{\mathcal{A}} \leq C_{rel} \eta_h + osc_h^{rel}.$$

Efficiency of the estimator guarantees the existence of $C_{eff} > 0$ independent of mesh size h such that

$$\eta_h \leq C_{eff} \|u - u_h\|_{\mathcal{A}} + osc_h^{eff}.$$

Our analysis assumes exact integration for the data of the problem and hence justifies the absence of the data oscillation terms.

The upper estimate on the error is mandatory for reliability, i.e. to ensure that the error is below a given tolerance. On the other hand, lower bounds for the error ensure that the required tolerance is achieved with a nearly minimal amount of work and thus, are indispensable for efficiency.

An estimator which is both reliable and efficient provides us with cheap and computable upper and lower estimates for the discretization error.

2.3 MARK

Based on a given parameter $\theta \in [0, 1]$, we set a threshold and select edges and elements (for refinement) whose indicators exceed this threshold.

There are several choices for setting this threshold for instance the marking of the elements/edges is controlled by the indicator of the largest magnitude (Maximum Strategy) or by an averaged indicator (Equidistribution Strategy). For other marking strategies, we refer to [12].

Our algorithm however, relies on the marking strategy introduced by Dörfler in [23] which will be explained in the following chapter.

2.4 REFINE

The final step refinement is realized by bisection i.e., each marked simplex is divided into atleast two subsimplices. There are different bisection methods which depend either upon the geometric structure of the triangulation (longest edge bisection) or are mainly concerned with the underlying topological structure (newest vertex bisection). The newest vertex bisection can be explained as below.

Given a marked triangle $T = span\{a_1, a_2, a_3\}$, we fix a vertex and label it as the newest vertex. The two children (elements) emanating from T share the new vertex

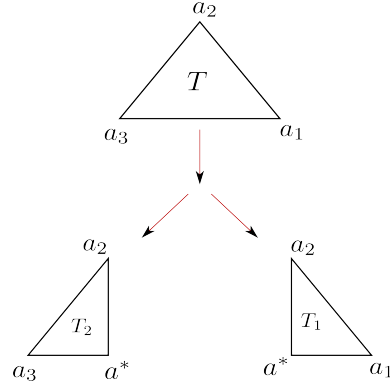


Figure 2.1: Newest vertex bisection: Assign one of the vertices as the new vertex a_2 , refinement is done by connecting a_2 to the midpoint a^* of the edge connecting a_1 and a_3 .

a_2 and are formed by splitting the edge opposite to this vertex. These children are ordered as $T_1 = \text{span}\{a_1, a^*, a_2\}$ and $T_2 = \text{span}\{a_3, a^*, a_2\}$.

The numerical implementation relies on the longest edge bisection. This bisection is a particular case of the newest vertex bisection wherein the newest vertex is fixed as the vertex that faces the longest edge. For a detailed explanation, we refer to [19] and references therein.

CHAPTER 3

Convergence Analysis

Finite element methods for acoustic wave propagation problems such as (3.1a)-(3.1c) have been widely studied in the literature (cf., e.g., [5, 18, 22, 37, 39] as well as the survey article [24], the monographs [36, 38] and the references therein). In case of large wavenumbers k , the finite element discretization typically requires fine meshes for a proper resolution of the waves and thus results in large linear algebraic systems to be solved. Moreover, the use of standard adaptive mesh refinement techniques based on a posteriori error estimators is marred by the pollution effect [8, 36]. Recently, Discontinuous Galerkin (DG) methods [21, 32, 44] have been increasingly applied to wave propagation problems in general [20] and the Helmholtz equation

in particular [3, 4, 25, 26, 27, 28] including hybridized DG approximations [30]. An a posteriori error analysis of DG methods for standard second-order elliptic boundary value problems has been performed in [2, 14, 16, 35, 40, 45], and a convergence analysis has been provided in [15, 34, 41]. However, to the best of our knowledge a convergence analysis for adaptive DG discretizations of the Helmholtz equation is not yet available in the literature.

It is the purpose of this chapter to provide such a convergence analysis for an Interior Penalty Discontinuous Galerkin (IPDG) discretization of (3.1a)-(3.1c) based on a residual-type a posteriori error estimator featuring element and edge residuals. This chapter is organized as follows:

In section 3.2, we introduce the adaptive IPDG method, discuss the consistency error due to the nonconformity of the approach, and present the residual a posteriori error estimator as well as the marking strategy (Dörfler marking) for adaptive mesh refinement. Section 3.3 shows that the consistency error can be controlled by the estimator, provides an estimator reduction property in the spirit of [17] and establishes the reliability of the estimator. Another important ingredient of the convergence analysis is a quasi-orthogonality result that will be dealt with in section 3.4. The particular difficulty we are facing here is the proper treatment of the lower order term in (3.1a) containing the wavenumber k . Adopting an idea from the convergence analysis of adaptive conforming edge element approximations of the time-harmonic Maxwell equation [49], we use the conforming approximation of (3.1a)-(3.1c) and take advantage of an Aubin-Nitsche type argument (cf. Lemma (3.4.4)). Hence, the quasi-orthogonality of the IPDG approximation can be established by invoking the

3.1. SCREEN PROBLEM

associated conforming approximations (cf. Theorem 3.4.1). Combining the reliability of the estimator, the estimator reduction property, and the quasi-orthogonality result, in section 3.5 we prove convergence of the adaptive IPDG in terms of a contraction property for a weighted sum of the discretization error in the mesh dependent energy norm and the error estimator.

3.1 Screen Problem

Let Ω_D and Ω_R be bounded polygonal domains in \mathbb{R}^2 such that $\Omega_D \subset \Omega_R$. We set $\Omega := \Omega_R \setminus \Omega_D$ and note that $\partial\Omega = \Gamma_D \cup \Gamma_R$ where $\Gamma_D := \partial\Omega_D$ and $\Gamma_R := \partial\Omega_R$. Given complex valued functions f in Ω and g on Γ_R , we consider the Helmholtz problem

$$-\Delta u - k^2 u = f \quad \text{in } \Omega, \tag{3.1a}$$

$$\frac{\partial u}{\partial \nu_R} + iku = g \quad \text{on } \Gamma_R, \tag{3.1b}$$

$$u = 0 \quad \text{on } \Gamma_D, \tag{3.1c}$$

which describes an acoustic wave with wavenumber $k > 0$ scattered at the sound-soft scatterer Ω_D . In (3.1b), ν_R denotes the exterior unit normal at Γ_R and i stands for the imaginary unit.

3.2 The IPDG Method

The functions considered in this paper are complex-valued. For a complex number $z \in \mathbb{C}$ we denote by $\operatorname{Re}(z), \operatorname{Im}(z)$ its real and imaginary part such that $z = \operatorname{Re}(z) + i\operatorname{Im}(z)$, $\bar{z} := \operatorname{Re}(z) - i\operatorname{Im}(z)$ is the complex conjugate of z and $|z| := \sqrt{\operatorname{Re}(z)^2 + \operatorname{Im}(z)^2}$ stands for the absolute value. We further adopt standard notation from Lebesgue and Sobolev space theory (cf., e.g., [48]). In particular, for $D \subseteq \Omega$ we refer to $L^2(D)$ and $H^s(D)$ as the Hilbert space of Lebesgue integrable complex-valued functions in D with inner product $(\cdot, \cdot)_{0,D}$ and associated norm $\|\cdot\|_{0,D}$ and the Sobolev space of complex-valued functions with inner product $(\cdot, \cdot)_{s,D}$ and norm $\|\cdot\|_{s,D}$. For $\Sigma \subseteq \partial D$ and a function $v \in H^s(D)$, we denote by $v|_{\Sigma}$ the trace of v on Σ .

Under the following assumption on the data of the problem

$$f \in L^2(\Omega), \quad g \in L^2(\Gamma_R), \quad (3.2)$$

the weak formulation of (3.1a)-(3.1c) amounts to the computation of $u \in V, V := H_{0,\Gamma_D}^1(\Omega) := \{v \in H^1(\Omega) \mid v|_{\Gamma_D} = 0\}$ such that for all $v \in V$ it holds

$$a(u, v) - k^2 c(u, v) + ik r(u, v) = \ell(v). \quad (3.3)$$

Here, the sesquilinear forms a, c, r and the linear functional ℓ are given by

$$\begin{aligned} a(u, v) &:= \int_{\Omega} \nabla u \cdot \nabla \bar{v} \, dx, & c(u, v) &:= \int_{\Omega} u \bar{v} \, dx, \\ r(u, v) &:= \int_{\Gamma_R} u \bar{v} \, ds, & \ell(v) &:= \int_{\Omega} f \bar{v} \, dx + \int_{\Gamma_R} g \bar{v} \, ds. \end{aligned}$$

3.2. THE IPDG METHOD

Remark 3.2.1 *It is well-known that (3.3) satisfies a Fredholm alternative (cf., e.g., [42]). In particular, if k^2 is not an eigenvalue of $-\Delta$ subject to the boundary conditions (3.1b),(3.1c), for any f, g satisfying (3.2) there exists a unique solution $u \in V$. In this case, the sesquilinear form $\hat{a}(\cdot, \cdot) := a(\cdot, \cdot) - k^2 c(\cdot, \cdot) + ikr(\cdot, \cdot)$ satisfies the inf-sup conditions*

$$\inf_{v \in V} \sup_{w \in V} \frac{|\hat{a}(v, w)|}{\|v\|_{1, \Omega} \|w\|_{1, \Omega}} = \inf_{w \in V} \sup_{v \in V} \frac{|\hat{a}(v, w)|}{\|v\|_{1, \Omega} \|w\|_{1, \Omega}} > \beta \quad (3.4)$$

hold true with a positive constant β depending only on Ω and on the wavenumber k .

For the formulation of the IPDG method, we assume \mathcal{H} to be a null sequence of positive real numbers and $(\mathcal{T}_h(\Omega))_{h \in \mathcal{H}}$ a shape-regular family of simplicial triangulations of Ω . For an element $T \in \mathcal{T}_h(\Omega)$, we denote by h_T the diameter of T and set $h := \max\{h_T \mid T \in \mathcal{T}_h(\Omega)\}$. For $D \subset \bar{\Omega}$, we refer to $\mathcal{E}_h(D)$ as the set of edges of $T \in \mathcal{T}_h(\Omega)$ in D . For $E \in \mathcal{E}_h(D)$, we denote by h_E the length of E and to $\omega_E := \bigcup\{T \in \mathcal{T}_H(\Omega) \mid E \subset \partial T\}$ as the patch consisting of the union of elements sharing E as a common edge. Moreover, $\mathcal{P}_N(D)$, $N \in \mathbb{N}$, stands for the set of complex-valued polynomials of degree $\leq N$ on D . In the sequel, for two mesh dependent quantities A and B we use the notation $A \lesssim B$, if there exists a constant $C > 0$ independent of h such that $A \leq CB$.

We introduce the finite element spaces

$$V_h := \{v_h : \bar{\Omega} \rightarrow \mathbb{C} \mid v_h|_T \in \mathcal{P}_N(T), T \in \mathcal{T}_H(\Omega)\}, \quad (3.5a)$$

$$\mathbf{V}_h := \{\mathbf{v}_h : \bar{\Omega} \rightarrow \mathbb{C}^2 \mid \mathbf{v}_h|_T \in \mathcal{P}_N(T)^2, T \in \mathcal{T}_H(\Omega)\}. \quad (3.5b)$$

Functions $v_h \in V_h$ are not continuous across interior edges $E \in \mathcal{E}_H(\Omega)$. For $E := T_+ \cap T_-, T_\pm \in \mathcal{T}_H(\Omega)$, we denote by $\{v_h\}_E$ the average of v_h on E and by $[v_h]_E$ the

3.2. THE IPDG METHOD

jump of v_h across E according to

$$\{v_h\}_E := \frac{1}{2}(v_h|_{E \cap T_+} + v_h|_{E \cap T_-}), \quad [v_h]_E := v_h|_{E \cap T_+} - v_h|_{E \cap T_-}, \quad E \in \mathcal{E}_h(\Omega),$$

and we define $\{v_h\}_E, [v_h]_E, E \in \mathcal{E}_h(\Gamma)$, accordingly.

We introduce a mesh dependent sesquilinear form $a_h^{IP} : V_h \times V_h \rightarrow \mathbb{C}$ by means of

$$\begin{aligned} a_h^{IP}(u_h, v_h) := & \sum_{T \in \mathcal{T}_h(\Omega)} (\nabla u_h, \nabla v_h)_{0,T} - \sum_{E \in \mathcal{E}_h(\Omega \cup \Gamma_D)} \left(\left\{ \frac{\partial u_h}{\partial \nu_E} \right\}_E, [v_h]_E \right)_{0,E} \\ & - \sum_{E \in \mathcal{E}_h(\Omega \cup \Gamma_D)} \left([u_h]_E, \left\{ \frac{\partial v_h}{\partial \nu_E} \right\}_E \right)_{0,E} + \sum_{E \in \mathcal{E}_h(\Omega \cup \Gamma_D)} \frac{\alpha}{h_E} ([u_h]_E, [v_h]_E)_{0,E}, \end{aligned} \quad (3.6)$$

where $\alpha > 0$ is a suitably chosen penalty parameter.

The IPDG method for the approximation of the solution of (3.1a)-(3.1c) requires the computation of $u_h \in V_h$ such that for all $v_h \in V_h$ it holds

$$a_h^{IP}(u_h, v_h) - k^2 c(u_h, v_h) + ik r(u_h, v_h) = \ell(v_h). \quad (3.7)$$

We further define $u_h^c \in V_h^c := V_h \cap H_{0,\Gamma_D}^1(\Omega)$ as the conforming finite element approximation of (3.1a)-(3.1c) satisfying

$$a(u_h^c, v_h^c) - k^2 c(u_h^c, v_h^c) + ik r(u_h^c, v_h^c) = \ell(v_h^c), \quad v_h^c \in V_h^c. \quad (3.8)$$

Remark 3.2.2 *If k^2 is not an eigenvalue of $-\Delta$ subject to the boundary conditions (3.1b),(3.1c), for sufficiently large penalty parameter α and sufficiently small mesh size h , the equations (3.7) and (3.8) have unique solutions $u_h \in V_h$ and $u_h^c \in V_h^c$ that continuously depend on the data. In particular, there exists $h^* \in \mathcal{H}, h^* \leq 1$, such*

3.2. THE IPDG METHOD

that for $h \leq h^*$ the sesquilinear forms $\hat{a}|_{V_h^c \times V_h^c}$ inherit (3.4), whereas the sesquilinear forms $\hat{a}_h^{IP}(\cdot, \cdot) := a_h^{IP}(\cdot, \cdot) - k^2 c(\cdot, \cdot) + ik r(\cdot, \cdot)$ satisfy analogues of (3.4) with positive inf-sup constants β_h being uniformly bounded away from zero. Moreover, (3.7) is consistent with (3.3) in the sense that the solution $u \in V$ of (3.3) satisfies (3.7) for $v_h = v_h^c \in V_h^c$. In the sequel, we will always assume that k^2 is not an eigenvalue of $-\Delta$ and h is sufficiently small such that (3.7) and (3.8) admit unique solutions.

We note that $a_h^{IP}(\cdot, \cdot)$ is not well defined on V . This can be remedied by means of a lifting operator $L : V + V_h \rightarrow \mathbf{V}_h$ according to

$$(L(v), \mathbf{v}_h)_{0,\Omega} := \sum_{E \in \mathcal{E}_h(\Omega \cup \Gamma_D)} ([v]_E, \nu_E \cdot \{\mathbf{v}_h\}_E)_{0,E}, \quad v \in V + V_h, \quad \mathbf{v}_h \in \mathbf{V}_h. \quad (3.9)$$

As has been shown, e.g., in [47], the lifting operator is stable in the sense that there exists a constant $C_L > 0$ depending only on the shape regularity of the triangulations such that

$$\|L(v)\|_{0,\Omega}^2 \leq C_L \sum_{E \in \mathcal{E}_h(\Omega \cup \Gamma_D)} h_E^{-1} \|[v]_E\|_{0,E}^2, \quad v \in V + V_h. \quad (3.10)$$

For completeness we provide a proof below:

Proof: In view of (3.9) and a straightforward application of the Cauchy Schwarz

3.2. THE IPDG METHOD

inequality yields

$$\begin{aligned}
 \|L(v)\|_{0,\Omega} &= \sup_{\mathbf{w} \in V_h^2} \frac{\left(\sum_{E \in \mathcal{E}_h(\Omega \cup \Gamma_D)} ([v]_E, \nu_E \cdot \{\mathbf{w}\}_E)_{0,E} \right)}{\|\mathbf{w}\|_{0,\Omega}} \\
 &\leq \sup_{\mathbf{w} \in V_h^2} \frac{\left(\sum_{E \in \mathcal{E}_h(\Omega \cup \Gamma_D)} h_E^{-1} \| [v]_E \|^2 \right)^{1/2} \left(\sum_{E \in \mathcal{E}_h(\Omega \cup \Gamma_D)} h_E \|\mathbf{w}\|_{0,E}^2 \right)^{1/2}}{\|\mathbf{w}\|_{0,\Omega}} \\
 &\leq \left(\sum_{E \in \mathcal{E}_h(\Omega \cup \Gamma_D)} h_E^{-1} \| [v]_E \|^2 \right)^{1/2} \sup_{\mathbf{w} \in V_h^2} \frac{\left(\sum_{T \in \mathcal{T}_h(\Omega)} C_L^2 \|\mathbf{w}\|_{0,T}^2 \right)^{1/2}}{\|\mathbf{w}\|_{0,\Omega}}
 \end{aligned}$$

where $C_L > 0$ depends upon the shape regularity of the triangulation. \square

Mesh Dependent Norms and their Equivalence

On $V + V_h$, we define the mesh dependent DG norm

$$\|v\|_{1,h,\Omega} := \left(\sum_{T \in \mathcal{T}_h(\Omega)} \|\nabla v\|_{0,T}^2 + \sum_{E \in \mathcal{E}_h(\Omega \cup \Gamma_D)} \alpha h_E^{-1} \| [v]_E \|^2 \right)^{1/2}, \quad (3.11)$$

It is well known (cf., e.g., [15] and the references therein) that for sufficiently large penalty parameter α , the DG-norm and the mesh dependent energy norm are equivalent. We provide the proof below for completeness.

Lemma 3.2.1 *There exist constants $\alpha_1 > 0$, $0 < \gamma < 1$, and $C_1 > 0$ such that for all $\alpha \geq \alpha_1$ and $v \in V + V_h$ it holds*

$$a_h^{IP}(v, v) \geq \gamma \|v\|_{1,h,\Omega}^2, \quad (3.12a)$$

3.2. THE IPDG METHOD

whereas for all $\alpha \geq 1$ and $v, w \in V + V_h$ we have

$$a_h^{IP}(v, w) \leq C_1 \|v\|_{1,h,\Omega} \|w\|_{1,h,\Omega}. \quad (3.12b)$$

Proof: For (3.12a), we can write $a_h^{IP}(v, v)$ as

$$\begin{aligned} a_h^{IP}(v, v) &= \sum_{T \in \mathcal{T}_h(\Omega)} \|\nabla v\|_{0,T}^2 - 2 \sum_{T \in \mathcal{T}_h(\Omega)} \operatorname{Re} (L(v), \nabla v)_{0,T} + \sum_{E \in \mathcal{E}_h(\Omega \cup \Gamma_D)} \alpha h_E^{-1} \|[v]_E\|_{0,E}^2 \\ &\geq \sum_{T \in \mathcal{T}_h(\Omega)} \|\nabla v\|_{0,T}^2 - 2 \left(C_L^2 \sum_{E \in \mathcal{E}_h(\Omega \cup \Gamma_D)} h_E^{-1} \|[v]_E\|_{0,E}^2 + \frac{1}{4} \sum_{T \in \mathcal{T}_h(\Omega)} \|\nabla v\|_{0,T}^2 \right) \\ &\quad + \sum_{E \in \mathcal{E}_h(\Omega \cup \Gamma_D)} \alpha h_E^{-1} \|[v]_E\|_{0,E}^2 \quad \text{using Young's inequality and (3.10)} \\ &= \frac{1}{2} \sum_{T \in \mathcal{T}_h(\Omega)} \|\nabla v\|_{0,T}^2 + (\alpha - 2C_L^2) \sum_{E \in \mathcal{E}_h(\Omega \cup \Gamma_D)} h_E^{-1} \|[v]_E\|_{0,E}^2. \end{aligned}$$

Setting $\alpha_1 = 4C_L^2$ and $\gamma = \frac{1}{2}$, and in view of (3.11) we conclude (3.12a).

Regarding the inequality (3.12b), a straightforward application of Cauchy-Schwarz inequality to each term in $a_h^{IP}(v, w)$ and using (3.10) gives us the required inequality.

□

The DG approach is a nonconforming finite element method, since V_h is not contained in $H_{0,\Gamma_D}^1(\Omega)$ due to the lack of continuity across interior edges $E \in \mathcal{E}_h(\Omega)$ and due to the enforcement of the homogeneous Dirichlet boundary condition (3.1c) by penalty terms on the edges $E \in \mathcal{E}_h(\Gamma_D)$. The nonconformity is measured by the consistency error

$$\xi := \inf_{v_h^c \in V_h^c} \left(\sum_{T \in \mathcal{T}_h(\Omega)} \|\nabla(u_h - v_h^c)\|_{0,T}^2 \right)^{1/2}. \quad (3.13)$$

3.2. THE IPDG METHOD

We refer to $\Pi_h^C : V_h \rightarrow V_h^c$ as the Clément-type quasi-interpolation operator introduced in [15] such that for some constant $C_A > 0$ depending only on the shape regularity of the triangulations it holds

$$\begin{aligned} \sum_{|\beta|} \sum_{T \in \mathcal{T}_h(\Omega)} \|D^\beta(u_h - \Pi_h^C u_h)\|_{0,T}^2 &\leq \\ C_A \sum_{E \in \mathcal{E}_h(\Omega \cup \Gamma_D)} h_E^{1-2|\beta|} \|[u_h]_E\|_{0,E}^2, \quad |\beta| \in \{0, 1\}. \end{aligned} \quad (3.14)$$

It follows from (3.14) that

$$\begin{aligned} \xi &\lesssim \eta_{h,c}, \\ \eta_{h,c} \equiv \eta_{h,c}(u_h) &:= \left(\sum_{E \in \mathcal{E}_h(\Omega \cup \Gamma_D)} \eta_{E,c}^2 \right)^{1/2}, \quad \eta_{E,c} := h_E^{-1/2} \|[u_h]_E\|_{0,E}. \end{aligned} \quad (3.15)$$

Lemma 3.2.2 *Let $u_h \in V_h$ and $u_h^c \in V_h^c$ be the solution of (3.7) and (3.8), respectively, and let $u_h^{nc} := u_h - u_h^c$. Then, for $\alpha \geq 1$ there exists a positive constant C_{nc} , depending on β, C_1 , and C_A , such that*

$$\sum_{T \in \mathcal{T}_h(\Omega)} \|u_h^{nc}\|_{1,T}^2 \leq C_{nc} \alpha \eta_{h,c}^2. \quad (3.16)$$

Proof: Obviously, we have

$$\sum_{T \in \mathcal{T}_h(\Omega)} \|u_h^{nc}\|_{1,T}^2 \leq 2 \sum_{T \in \mathcal{T}_h(\Omega)} \left(\|u_h - \Pi_h^C u_h\|_{1,T}^2 + \|u_h^c - \Pi_h^C u_h\|_{1,T}^2 \right). \quad (3.17)$$

It follows from (3.8) that $u_h^c - \Pi_h^C u_h$ satisfies

$$\hat{a}(u_h^c - \Pi_h^C u_h, v_h^c) = \ell(v_h^c) - \hat{a}(\Pi_h^C u_h, v_h^c), \quad v_h^c \in V_h^c.$$

3.3. A POSTERIORI ERROR ANALYSIS

Hence, in view of Remark 3.2.2 there exists a positive constant C_β such that

$$\|u_h^c - \Pi_h^C u_h\|_{1,\Omega} \leq C_\beta \sup_{v_h^c \neq 0} \frac{|\ell(v_h^c) - \hat{a}(\Pi_h^C u_h, v_h^c)|}{\|v_h^c\|_{1,\Omega}}. \quad (3.18)$$

Since u_h satisfies (3.7) for $v_h = v_h^c$ and $\hat{a}_h|_{V_h^c \times V_h^c} = \hat{a}|_{V_h^c \times V_h^c}$, it holds

$$\ell(v_h^c) - \hat{a}(\Pi_h^C u_h, v_h^c) = \hat{a}_h(u_h - \Pi_h^C u_h, v_h^c). \quad (3.19)$$

Using (3.19) in (3.18) as well as (3.12b), we find

$$\|u_h^c - \Pi_h^C u_h\|_{1,\Omega} \leq C_\beta C_1 \|u_h - \Pi_h^C u_h\|_{1,h,\Omega}. \quad (3.20)$$

The assertion then follows from (3.17), (3.20), and (3.14). \square

3.3 A Posteriori Error Analysis

We consider the residual-type a posteriori error estimator

$$\eta_h := \left(\sum_{T \in \mathcal{T}_h(\Omega)} \eta_T^2 + \sum_{E \in \mathcal{E}_h(\Omega \cup \Gamma_D)} \eta_{E,1}^2 + \sum_{E \in \mathcal{E}_h(\Gamma_R)} \eta_{E,2}^2 \right)^{1/2}, \quad (3.21)$$

consisting of the element residuals

$$\eta_T := h_T \|f + \Delta u_h + k^2 u_h\|_{0,T}, \quad T \in \mathcal{T}_h(\Omega), \quad (3.22)$$

and the edge residuals

$$\eta_{E,1} := h_E \left\| \left[\frac{\partial u_h}{\partial \nu_E} \right]_E \right\|_{0,E}, \quad E \in \mathcal{E}_h(\Omega \cup \Gamma_D), \quad (3.23a)$$

$$\eta_{E,2} := h_E \left\| g - \frac{\partial u_h}{\partial \nu_E} - i k u_h \right\|_{0,E}, \quad E \in \mathcal{E}_h(\Gamma_R). \quad (3.23b)$$

3.3. A POSTERIORI ERROR ANALYSIS

As marking strategy for refinement we use Dörfler marking [23], i.e., given a constant $0 < \theta < 1$, we compute a set \mathcal{M}_1 of elements $T \in \mathcal{T}_h(\Omega)$ and a set \mathcal{M}_2 of edges $E \in \mathcal{E}_h(\bar{\Omega})$ such that

$$\theta \eta_h \leq \tilde{\eta}_h := \left(\sum_{T \in \mathcal{M}_1} \eta_T^2 + \sum_{E \in \mathcal{M}_2} (\eta_{E,1}^2 + \eta_{E,2}^2) \right)^{1/2}. \quad (3.24)$$

Once the sets $\mathcal{M}_i, 1 \leq i \leq 2$, have been determined, a refined triangulation is generated based on newest vertex bisection [46].

The following result shows that the upper bound for the consistency error can be controlled by the error estimator (cf. [15]). The proof follows the arguments of Lemma 3.6 in [15], but will be given for completeness.

Lemma 3.3.1 *There exists a constant $C_J > 0$, depending only on the shape regularity of $\mathcal{T}_h(\Omega)$, such that for $\alpha \geq \alpha_2 := 2C_J/\gamma$ it holds*

$$\alpha \eta_{h,c}^2 \leq 2 \frac{C_J}{\gamma} \eta_h^2. \quad (3.25)$$

Proof: In view of (3.12a) and (3.7) with $v_h = u_h - \Pi_h^C u_h$, we obtain

$$\begin{aligned} \alpha \eta_{h,c}^2 &\leq \|u_h - \Pi_h^C u_h\|_{1,h,\Omega}^2 \leq \gamma^{-1} a_h^{IP}(u_h - \Pi_h^C u_h, u_h - \Pi_h^C u_h) \\ &= \gamma^{-1} \left(\sum_{T \in \mathcal{T}_h(\Omega)} (f + k^2 u_h, u_h - \Pi_h^C u_h)_{0,T} \right. \\ &\quad \left. + \sum_{E \in \mathcal{E}_h(\Gamma_R)} (g - ik u_h, u_h - \Pi_h^C u_h)_{0,E} - a_h^{IP}(\Pi_h^C u_h, u_h - \Pi_h^C u_h) \right). \end{aligned} \quad (3.26)$$

Observing $L(\Pi_h^C u_h) = 0$, $[\Pi_h^C u_h]_E = 0$, for the last term on the right-hand side of

3.3. A POSTERIORI ERROR ANALYSIS

(3.26) it follows that

$$\begin{aligned}
 a_h^{IP}(\Pi_h^C u_h, u_h - \Pi_h^C u_h) &= \sum_{T \in \mathcal{T}_h(\Omega)} (\nabla \Pi_h^C u_h, \nabla(u_h - \Pi_h^C u_h))_{0,T} \\
 &- \sum_{T \in \mathcal{T}_h(\Omega)} \overline{(L(u_h), \nabla \Pi_h^C u_h)}_{0,T} = \sum_{T \in \mathcal{T}_h(\Omega)} (\nabla u_h, \nabla(u_h - \Pi_h^C u_h))_{0,T} \\
 &- \sum_{T \in \mathcal{T}_h(\Omega)} \|\nabla(u_h - \Pi_h^C u_h)\|_{0,T}^2 - \sum_{T \in \mathcal{T}_h(\Omega)} \overline{(L(u_h), \nabla(\Pi_h^C u_h))}_{0,T}.
 \end{aligned} \tag{3.27}$$

An elementwise application of Green's formula reveals

$$\begin{aligned}
 a_h^{IP}(\Pi_h^C u_h, u_h - \Pi_h^C u_h) &= \sum_{T \in \mathcal{T}_h(\Omega)} (-\Delta u_h, u_h - \Pi_h^C u_h)_{0,T} \\
 &+ \sum_{E \in \mathcal{E}_h(\Omega \cup \Gamma_D)} (\nu_E \cdot [\nabla u_h]_E, \{u_h - \Pi_h^C u_h\}_E)_{0,E} + \sum_{E \in \mathcal{E}_h(\Gamma_R)} (g - ik u_h, u_h - \Pi_h^C u_h)_{0,E} \\
 &- \sum_{T \in \mathcal{T}_h(\Omega)} \|\nabla(u_h - \Pi_h^C u_h)\|_{0,T}^2 + \sum_{T \in \mathcal{T}_h(\Omega)} \overline{(L(u_h), \nabla(u_h - \Pi_h^C u_h))}_{0,T}.
 \end{aligned} \tag{3.28}$$

Using (3.27) and (3.28) in (3.26), straightforward estimation yields

$$\begin{aligned}
 a_h^{IP}(u_h - \Pi_h^C u_h, u_h - \Pi_h^C u_h) &\lesssim \eta_h \left(\left(\sum_{T \in \mathcal{T}_h(\Omega)} h_T^{-1} \|u_h - \Pi_h^C u_h\|_{0,T}^2 \right)^{1/2} \right. \\
 &+ \left(\sum_{E \in \mathcal{E}_h(\Omega \cup \Gamma_D)} h_E^{-1} \|u_h - \Pi_h^C u_h\|_{0,E}^2 \right)^{1/2} + \sum_{T \in \mathcal{T}_h(\Omega)} \|\nabla(u_h - \Pi_h^C u_h)\|_{0,T}^2 \\
 &\left. + \left(\sum_{T \in \mathcal{T}_h(\Omega)} \|L(u_h)\|_{0,T}^2 \right)^{1/2} \left(\sum_{T \in \mathcal{T}_h(\Omega)} \|\nabla(u_h - \Pi_h^C u_h)\|_{0,T}^2 \right)^{1/2}.
 \end{aligned} \tag{3.29}$$

The stability (3.10) of the extension operator L and the local approximation properties (3.14) of Π_h^C imply the existence of $C_J > 0$ such that

$$\alpha \eta_{h,c}^2 \leq \frac{C_J}{\gamma} \left(\eta_h^2 + \eta_{h,c}^2 \right), \tag{3.30}$$

which readily leads to the assertion. \square

As a by-product of the preceding lemma we obtain the following results:

3.3. A POSTERIORI ERROR ANALYSIS

Corollary 3.3.1 *Let $u_h \in V_h$ be the IPDG solution of (3.7), let $u_h^c \in V_h^c$ be the solution of (3.8), and let $u_h^{nc} := u_h - u_h^c$. Then, there exists a constant $C_{ce} > 0$, depending on γ, C_γ , and C_J , such that*

$$\|u_h^{nc}\|_{1,h,\Omega}^2 \leq \frac{C_{ce}}{\alpha} \eta_h^2. \quad (3.31)$$

Proof: With $C_{ce} := (2(1 + C_{nc}C_J)/\gamma)$ the assertion is an immediate consequence of Lemma 3.2.2 and Lemma 3.3.1. \square

Corollary 3.3.2 *Let $\mathcal{T}_h(\Omega)$ be a simplicial triangulation obtained by refinement from $\mathcal{T}_H(\Omega)$, and let $u_h \in V_h$, $u_H \in V_H$ and η_h, η_H be the associated IPDG solutions of (3.7) and error estimators, respectively. Moreover, let $u_h^c \in V_h^c$ and $u_H^c \in V_H^c$ be the conforming approximations of (3.1a)-(3.1c) according to (3.8). Then, for $u_h^{nc} := u_h - u_h^c$ and $u_H^{nc} := u_H - u_H^c$ we have*

$$\|u_h^{nc} - u_H^{nc}\|_{1,h,\Omega}^2 \leq 4 \frac{C_{ce}}{\alpha} (\eta_h^2 + \eta_H^2). \quad (3.32)$$

Proof: The triangle inequality yields

$$\|u_h^{nc} - u_H^{nc}\|_{1,h,\Omega}^2 \leq 2 \left(\|u_h^{nc}\|_{1,h,\Omega}^2 + \|u_H^{nc}\|_{1,h,\Omega}^2 \right). \quad (3.33)$$

Taking

$$\sum_{E \in \mathcal{E}_h} \frac{1}{h_E} \|[u_H^{nc}]_E\|_{0,E}^2 \leq 2 \sum_{E \in \mathcal{E}_H} \frac{1}{H_E} \|[u_H^{nc}]_E\|_{0,E}^2$$

3.3. A POSTERIORI ERROR ANALYSIS

into account and using Corollary 3.3.1 with h replaced by H , we find

$$\|u_H^{nc}\|_{1,h,\Omega}^2 \leq 2 \frac{C_{ce}}{\alpha} \eta_H^2. \quad (3.34)$$

We conclude by using (3.32) and (3.34) in (3.33). \square

The residual estimator η_h has the following monotonicity property

$$\eta_h \leq \eta_H \quad (3.35)$$

for all refinements $\mathcal{T}_h(\Omega)$ of $\mathcal{T}_H(\Omega)$. The latter can be used to prove the following estimator reduction result which will be strongly used for the contraction property in section 3.5.

Lemma 3.3.2 *Let $\mathcal{T}_h(\Omega)$ be a simplicial triangulation obtained by refinement from $\mathcal{T}_H(\Omega)$, and let $u_h \in V_h, u_H \in V_H$, and $\eta_h, \eta_H, \tilde{\eta}_H$ be the associated IPDG solutions and error estimators, respectively. Then, for any $\tau > 0$ there exists a constant $C_\tau > 0$, depending only on the shape regularity of the triangulations, such that*

$$\eta_h^2 \leq (1 + \tau) \left(\eta_H^2 - (1 - 2^{-1/2}) \tilde{\eta}_H^2 \right) + C_\tau \sum_{T \in \mathcal{T}_h(\Omega)} \|\nabla(u_h - u_H)\|_{0,T}^2. \quad (3.36)$$

Proof: The proof can be done along the same lines as the proof of Corollary 3.4 in [17].

For $T \in \mathcal{T}_h(\Omega)$, we set the following notation:

$$\eta_h^2(u_h, T) := \eta_T^2(u_h) + \sum_{E \in \mathcal{E}(T) \cup \mathcal{E}(T \cap \Gamma_D)} \eta_{E,1}^2(u_h) + \sum_{E \in \mathcal{E}(T) \cup \mathcal{E}(T \cap \Gamma_R)} \eta_{E,2}^2(u_h)$$

3.3. A POSTERIORI ERROR ANALYSIS

where the element and edge residuals are:

$$\begin{aligned}\eta_T(u_h) &:= h_T \|f + \Delta u_h + k^2 u_h\|_{0,T}, \\ \eta_{E,1}(u_h) &:= h_E \left\| \left[\frac{\partial u_h}{\partial \nu_E} \right]_E \right\|_{0,E}, \quad E \in \mathcal{E}(T) \cup \mathcal{E}(T \cap \Gamma_D), \\ \eta_{E,2}(u_h) &:= h_E \left\| g - \frac{\partial u_h}{\partial \nu_E} - ik u_h \right\|_{0,E}, \quad E \in \mathcal{E}(T) \cup \mathcal{E}(T \cap \Gamma_R).\end{aligned}$$

By a straightforward application of the triangle's inequality, we have:

$$\begin{aligned}\eta_T(u_h, T) &\leq \eta_T(u_H, T) + h_T \|\Delta w + \kappa^2 w\|_{0,T} + \sum_{E \in \mathcal{E}(T) \cup \mathcal{E}(T \cap \Gamma_D)} h_E \left\| \left[\frac{\partial w}{\partial \nu_E} \right]_E \right\|_{0,E} \\ &\quad + \sum_{E \in \mathcal{E}(T) \cup \mathcal{E}(T \cap \Gamma_R)} h_E \left\| \frac{\partial w}{\partial \nu_E} + ikw \right\|_{0,E} \quad \text{where } w = u_h - u_H.\end{aligned}$$

By invoking local inverse estimates for the edge and element terms, we can find a constant $C \equiv C(k, \Omega) > 0$ such that the following estimate:

$$\eta_T(u_h, T) \leq \eta_T(u_H, T) + C \sum_{T^* \in w_E} \|\nabla(u_h - u_H)\|_{0,T^*}$$

holds.

Now,

$$\begin{aligned}\eta_T^2(u_h, T) &\leq \eta_T^2(u_H, T) + 2C \eta_T(u_H, T) \sum_{T^* \in w_E} \|\nabla(u_h - u_H)\|_{0,T^*} \\ &\quad + C^2 \left(\sum_{T^* \in w_E} \|\nabla(u_h - u_H)\|_{0,T^*} \right)^2 \\ &\leq (1 + \tau) \eta_T^2(u_H, T) + (1 + \tau^{-1}) C^2 \left(\sum_{T^* \in w_E} \|\nabla(u_h - u_H)\|_{0,T^*} \right)^2\end{aligned}$$

using Young's inequality with constant $\tau > 0$.

Futhermore, summing over all the elements, employing the finite overlap property of patches w_T , we obtain

$$\eta_h^2(u_h, \mathcal{T}_h) \lesssim (1 + \tau) \eta_h^2(u_H, \mathcal{T}_h) + C (1 + \tau^{-1}) \sum_{T \in \mathcal{T}_h(\Omega)} \|\nabla(u_h - u_H)\|_{0,T}^2. \quad (3.37)$$

3.3. A POSTERIORI ERROR ANALYSIS

For $T_H \in \mathcal{T}_H$,

set

$$\mathcal{M}_h(T_H) := \{T \in \mathcal{T}_h | T \subset T_H\} \quad \text{and} \quad \mathcal{M}_h := \bigcup_{T_H \in \mathcal{T}_H} \mathcal{M}_h(T_H).$$

As a consequence of refinement by bisection,

$$\sum_{T \in \mathcal{M}_h(T_H)} \eta_h^2(u_H, T) \leq 2^{-1/2} \eta_H^2(u_H, T_H). \quad (*)$$

Obviously, $\mathcal{T}_h \setminus \mathcal{M}_h = \mathcal{T}_H \setminus \mathcal{M}$, where \mathcal{M} is the collection of elements and edges in \mathcal{T}_H which are marked for refinement.

Thus in view of (*),

$$\begin{aligned} \eta_h^2(u_H, \mathcal{T}_h) &= \sum_{T \in \mathcal{T}_h \setminus \mathcal{M}_h} \eta_h^2(u_H, T) + \sum_{T \in \mathcal{M}_h} \eta_h^2(u_H, T) \\ &\leq \sum_{T \in \mathcal{T}_H \setminus \mathcal{M}} \eta_h^2(u_H, T) + 2^{-1} \sum_{T \in \mathcal{M}} \eta_h^2(u_H, T) \\ &\leq \sum_{T \in \mathcal{T}_H} \eta_h^2(u_H, T) - (1 - 2^{-1}) \sum_{T \in \mathcal{M}} \eta_h^2(u_H, T). \end{aligned}$$

Replacing $\eta_h^2(u_H, \mathcal{T}_h)$ in (3.37) by the upper bound obtained above, we can conclude (3.36). \square

Corollary 3.3.3 *Under the same assumptions as in Lemma 3.3.2 let $\tau(\theta) := (1 + \tau)(1 - 2^{-1/2})\theta$ with θ from (3.24). Then, it holds*

$$\eta_h^2 \leq \tau(\theta) \eta_H^2 + C_\tau \sum_{T \in \mathcal{T}_h(\Omega)} \|\nabla(u_h - u_H)\|_{0,T}^2. \quad (3.38)$$

3.3. A POSTERIORI ERROR ANALYSIS

The proof is a direct consequence of (3.24) and (3.36).

In the next couple of subsections, we establish the reliability and efficiency of the estimator which essentially allows us to conclude the equivalence of the discretization error in the DG norm and the estimator.

We have assumed the exact integration for the data of the problem and as a result the data oscillation terms which arose in [15], [34], and [41] donot appear in our estimates.

3.3.1 Reliability

Theorem: Let $u \in V$ and $u_h \in V_h$ be the solution of (3.3) and (3.7), respectively, and let ξ and $\eta_h, \eta_{h,C}$ be the consistency error, the a posteriori error estimator, and the jump term as given by (3.13),(3.21), and (3.15). Then, there exists a constant $C_{rel} > 0$, depending only on the shape regularity of the triangulations and the wave number κ , such that there holds

$$a_h^{IP}(u - u_h, u - u_h) \leq C_{rel} \eta_h^2. \quad (3.39)$$

Proof: The discrete analogue of (3.4) implies

$$\begin{aligned} \|u - u_h\|_{1,h,\Omega} &\leq \beta^{-1} \sup_{0 \neq v_h \in V_h} \frac{|\hat{a}_h^{IP}(v_h, u - u_h)|}{\|v_h\|_{1,h,\Omega}} \\ &\leq C \hat{a}_h^{IP}(u - u_h, u - u_h)^{1/2}. \end{aligned}$$

3.3. A POSTERIORI ERROR ANALYSIS

And as a consequence of (3.12b) ,

$$a_h^{IP}(u - u_h, u - u_h) \lesssim \hat{a}_h^{IP}(u - u_h, u - u_h). \quad (3.40)$$

In the remainder of this proof, we show that $C_{rel} \eta_h^2$ is an upper estimates for

$$\hat{a}_h^{IP}(u - u_h, u - u_h) .$$

To this end, we follow the same approach as in ([15], Lemma 3.1) which involves decomposing $u_h \in V_h$ as

$$u_h = u_h^c + u_h^{nc}$$

where $u_h^{nc} = u_h - u_h^c$ denotes the $\hat{a}_h^{IP}(\cdot, \cdot)$ -orthogonal complement of $u_h^c \in V_h^c$ in V_h , and considering

$$\begin{aligned} \hat{a}_h^{IP}(u - u_h, u - u_h) &= \hat{a}_h^{IP}(u - u_h, u - u_h^c - u_h^{nc}) \\ &= \hat{a}_h^{IP}(u - u_h, v - \pi_h^c v) + \hat{a}_h^{IP}(u - u_h, \pi_h^c v) - \hat{a}_h^{IP}(u - u_h, u_h^{nc}) \\ &= \hat{a}_h^{IP}(u - u_h, v - \pi_h^c v) - \hat{a}_h^{IP}(u - u_h, u_h^{nc}) \text{ where } v = u - u_h^c \in V. \end{aligned}$$

By applying the Green's formula elementwise,

$$\begin{aligned} \hat{a}_h^{IP}(u - u_h, v - \pi_h^c v) &= \sum_{T \in \mathcal{T}_h(\Omega)} (f + \Delta u_h + \kappa^2 u_h, v - \pi_h^c v)_{0,T} \\ &\quad - \sum_{E \in \mathcal{E}_h(\Omega \cup \Gamma_D)} (\nu_E \cdot [\nabla u_h]_E, v - \pi_h^c v)_{0,E} \\ &\quad + \sum_{E \in \mathcal{E}_h(\Gamma_R)} (g - \partial u / \partial_E \nu - i\kappa u, v - \pi_h^c v)_{0,E} \\ &\quad - \sum_{T \in \mathcal{T}_h(\Omega)} (L(u_h), \nabla(v - \pi_h^c v))_{0,T}. \end{aligned}$$

3.3. A POSTERIORI ERROR ANALYSIS

Observing that

$$\begin{aligned}
 \|u_h^{nc}\|^2 &\leq \frac{1}{\gamma} a_h^{IP}(u_h^{nc}, u_h^{nc}) \\
 &= \frac{1}{\gamma} \inf_{w_h^c \in V_h^c} a_h^{IP}(u_h - w_h^c, u_h^c - w_h^c) \\
 &\leq \frac{1}{\gamma} a_h^{IP}((u_h - \pi_h^c u_h), u_h - \pi_h^c u_h) \\
 &\leq \frac{C_1}{\gamma} \|u_h - \pi_h^c u_h\|^2,
 \end{aligned}$$

the second term becomes

$$\begin{aligned}
 \hat{a}_h^{IP}(u - u_h, u_h^{nc}) &\leq \hat{a}_h^{IP}(u - u_h, u - u_h)^{1/2} \|u_h^{nc}\| \\
 &\leq \frac{1}{4} \hat{a}_h^{IP}(u - u_h, u - u_h) + \|u_h^{nc}\|^2 \\
 &\leq \frac{1}{4} \hat{a}_h^{IP}(u - u_h, u - u_h) + C \xi^2,
 \end{aligned}$$

following a simple application of Young's inequality.

Collecting all the upper bounds obtained, allows us to conclude the reliability of the estimator. \square

3.3.2 Efficiency

We provide a lower bound for the discretization error in terms of the estimator η_h .

For this purpose, we make use of bubble functions associated with the edges and triangles of $\mathcal{T}_h(\Omega)$.

For a given triangle $T \in \mathcal{T}_h(\Omega)$ with barycentric coordinates λ_i $1 \leq i \leq 3$, we define

3.3. A POSTERIORI ERROR ANALYSIS

a **triangle-bubble function** ψ_T as

$$\psi_T := 27 \lambda_1 \lambda_2 \lambda_3.$$

It is obvious that the support of ψ_T resides in the interior of T and that within T , ψ_T is positive with $\|\psi_T\|_\infty = 1$.

Also, for an edge $E \in \partial T$ associated with the barycentric coordinates λ_1, λ_2 , we introduce an **edge bubble function** ψ_E according as:

$$\psi_E := 4 \lambda_1 \lambda_2.$$

Extension of ψ_E to T : Clearly, for any other edge $E' \in \partial T$, $\psi_E|_{E'} = 0$. Furthermore, function p_E defined on the edge E can be extended to p_T whole triangle T by associating to every $x \in T$, a unique $x_E \in E$ such that $x - x_E$ is parallel to a fixed edge $E' \neq E$ and satisfies $p_T(x) = p_E(x_E)$.

Theorem: Let $\mathcal{T}_h(\Omega)$ be a triangulation of Ω and suppose that $u \in V$ and $u_h \in V_h$ are solutions to (3.3) and (3.7), respectively.

Then, there exists $C_e > 0$ depending on the shape regularity of the mesh and the wave number κ such that:

$$C_e \eta_h^2 \lesssim \|u - u_h\|_{1,h,\Omega}^2$$

Proof: The proof is in the same spirit as [Theorem 3.2, [40]] which involves establishing the local efficiency for the element and edge residuals.

We invoke the bubble function ψ_T with support in $T \in \mathcal{T}(\Omega)$, and observe that since

3.3. A POSTERIORI ERROR ANALYSIS

$\psi_T > 0$ on the interior of T , $\left(\int_T (\cdot)^2 \psi_T\right)^{1/2}$ can be thought of as a norm on $L^2(T)$ which is equivalent to the L^2 -norm on T thereby guaranteeing the existence of a constant $C > 0$ such that

$$C \int_T (f + \Delta u_h + \kappa^2 u_h)^2 dx \leq \int_T (f + \Delta u_h + \kappa^2 u_h)^2 \psi_T dx$$

holds.

An application of Green's formula reveals,

$$\begin{aligned}
 & \int_T \underbrace{(f + \Delta u_h + \kappa^2 u_h)^2}_{p_h} \psi_T dx \\
 &= \int_T f p_h \psi_T dx + \int_T \Delta u_h (p_h \psi_T) dx + \kappa^2 \int_K u_h (p_h \psi_T) dx \\
 &= \int_T -(\Delta u + \kappa^2 u)(p_h \psi_T) dx - \int_T \nabla u_h \nabla (p_h \psi_T) dx + \\
 & \quad \kappa^2 \int_K u_h (p_h \psi_T) dx \\
 &= \int_T \nabla(u - u_h) \nabla (p_h \psi_T) dx - \kappa^2 \int_T (u - u_h)(p_h \psi_T) dx.
 \end{aligned}$$

We now obtain upper estimates for each of these terms. Using Young's inequality and an inverse inequality, we have

$$\begin{aligned}
 \int_T \nabla(u - u_h) \nabla (p_h \psi_T) dx &\leq \|\nabla(u - u_h)\|_T \|\nabla(p_h \psi_T)\|_T \\
 &\leq \frac{1}{2\varepsilon h_T^2} \|\nabla(u - u_h)\|_T^2 + \frac{C\varepsilon}{2} \|p_h \psi_T\|_T^2
 \end{aligned}$$

$$\kappa^2 (u - u_h, p_h \psi_T) \leq \frac{\kappa^2 c}{2\varepsilon h_T^2} \|\nabla(u - u_h)\|_T^2 + \frac{C\varepsilon}{2} \|p_h \psi_T\|_T^2.$$

Thus taking $\varepsilon = 1/2$, we obtain

$$h_T^2 \int_T (f + \Delta u_h + \kappa^2 u_h)^2 dx \leq 4\kappa^2 \|\nabla(u - u_h)\|_T^2.$$

3.3. A POSTERIORI ERROR ANALYSIS

Regarding the edge residuals, we consider the bubble function ψ_E associated with the interior edge E shared by the two elements T_1 and T_2 and naturally extend ψ_E to $\psi_{T_1 \cup T_2}$ defined over $T_1 \cup T_2$. We also extend $[\frac{\partial u_h}{\partial \nu_E}]_E$ to $T_1 \cup T_2$ via the function ϕ which is defined as follows,

$$\phi(x) = [\frac{\partial u_h}{\partial \nu_E}]_E \phi_E(x_E)$$

with ϕ_E denoting a linear function that associates to every $x \in T$, a unique x_E on E satisfying

$$\inf_{x'_E \in E} d(x, x_E) = d(x, x'_E)$$

with d denoting the Euclidean metric on T . In other words, ϕ_E extends along the normals to E .

Associated with $T_1 \cup T_2$, we use the following inequality which states that for any $w \in H_0^1(\Omega)$, there holds

$$h_E \|w\|_{0, T_1 \cup T_2}^2 \lesssim \sum_{i=1}^2 h_{T_i} \|w\|_{0, T_i}^2. \quad (*)$$

The following inequality (***) holds as a consequence of the definition of ϕ ,

$$\|\phi^2\|_T = \int_E [\frac{\partial u_h}{\partial \nu_E}]_E^2 \phi_E(x_E)^2 dx_E \leq h_E \|[\frac{\partial u_h}{\partial \nu_E}]_E\|_{0, E}^2. \quad (***)$$

3.3. A POSTERIORI ERROR ANALYSIS

Set $v = \psi_{T_1 \cup T_2} \phi$ and in view of (*) we have,

$$\begin{aligned}
 h_E \int_E \left| \left[\frac{\partial u_h}{\partial \nu_E} \right]_E \right|^2 ds &= h_E \left(\int_{T_1 \cup T_2} (f + \Delta u_h + \kappa^2 u_h) \bar{v} dx - \int_{T_1 \cup T_2} \nabla(u - u_h) \nabla \bar{v} dx \right. \\
 &\quad \left. + \kappa^2 \int_{T_1 \cup T_2} (u - u_h) \bar{v} dx \right) \\
 &\leq \sum_{i=1}^2 \frac{\varepsilon^{-1}}{2} \left(h_{T_i}^2 \|f + \Delta u_h + \kappa^2 u_h\|_{0, T_i}^2 + \kappa^2 \|u - u_h\|_{0, T_i}^2 + \right. \\
 &\quad \left. \|\nabla(u - u_h)\|_{0, T_i}^2 \right) + \frac{\varepsilon}{2} \sum_{i=1}^2 \left((1 + \kappa^2) \|v\|^2 + \|\nabla v\|^2 \right).
 \end{aligned}$$

Once again we take advantage of the following equivalence of the L^2 -norm on E and the weighted norm $\left(\int_E (\cdot)^2 \psi_E \right)^{1/2}$

$$c \left\| \frac{\partial u_h}{\partial \nu_E} \right\|_{0, E}^2 \leq \int_E \left[\frac{\partial u_h}{\partial \nu_E} \right]^2 \psi_E ds$$

and use the following upper bound which is established using (**)

$$\|v\|^2 = \|\psi_{T_1 \cup T_2} \phi\|^2 \leq \|\phi\|^2 \lesssim h_E \left\| \left[\frac{\partial u_h}{\partial \nu_E} \right]_E \right\|_{0, E}^2$$

as well as an inverse inequality to obtain

$$h_E \left\| \left[\frac{\partial u_h}{\partial \nu_E} \right]_E \right\|_{0, E}^2 \lesssim \sum_{i=1}^2 \|\nabla(u - u_h)\|_{0, T_i}^2.$$

Similarly, if E is an edge living on the Dirichlet part of the boundary Γ_D , we follow the same argument as above with the convention that $\left[\frac{\partial u_h}{\partial \nu_E} \right]_E = \frac{\partial u_h}{\partial \nu_E}$ to obtain

$$h_E \left\| \left[\frac{\partial u_h}{\partial \nu_E} \right]_E \right\|_{0, E}^2 \lesssim \|\nabla(u - u_h)\|_{0, T}^2.$$

3.4. QUASI-ORTHOGONALITY

Lastly, for edges on the boundary Γ_R of the exterior domain, we use the edge bubble function ψ_E associated with E and set

$$v = (g - i\kappa u_h - \frac{\partial u_h}{\partial \nu_E})_{\tilde{T}} \psi_{\tilde{T}}$$

where $\psi_{\tilde{T}}$ denotes the extension of ψ_E to the element T containing the edge E and letting $(g - i\kappa u_h - \frac{\partial u_h}{\partial \nu_E})_{\tilde{T}}$ denote the extension of $(g - i\kappa u_h - \frac{\partial u_h}{\partial \nu_E})$ to T so that the local residual can be represented as

$$\begin{aligned} h_E \left\| g - i\kappa u_h - \frac{\partial u_h}{\partial \nu_E} \right\|_E^2 &= h_E \left(\int_T \nabla(u - u_h) \nabla \bar{v} \, dx - \int_T (f + \Delta u_h + \kappa^2 u_h) \bar{v} \, dx \right. \\ &\quad \left. - \kappa^2 \int_T (u - u_h) \bar{v} \, dx + i\kappa \int_E (u - u_h) \bar{v} \, ds \right). \end{aligned}$$

We use the same estimates as before to obtain an upper bound in terms of

$$\|\nabla(u - u_h)\|_{0,T}^2. \square$$

3.4 Quasi-orthogonality

Besides the reliability of the estimator and the estimator reduction result, a quasi-orthogonality property is a further important ingredient of the convergence analysis (cf. [15, 41, 34]). Here, the derivation of such a property is complicated due to the presence of the lower order term in the Helmholtz equation (3.1a). Adopting an idea from [29] (cf. also [49]) for the time-harmonic Maxwell equations, we resort to an Aubin-Nitsche type argument for the associated conforming approximation of the screen problem. As will be seen below, this additionally involves the error between the IPDG approximation and its conforming counterpart.

3.4. QUASI-ORTHOGONALITY

3.4.1 Mesh Perturbation Result

In the convergence analysis of IPDG methods for second-order elliptic boundary value problems, mesh perturbation results estimating the coarse mesh error in the fine mesh energy norm from above by its coarse mesh energy norm have played a central role in the convergence analysis as a prerequisite for establishing a quasiorthogonality result (cf., e.g., [15, 34, 41]). Here, we provide the following mesh perturbation result:

Lemma 3.4.1 *Let $\mathcal{T}_h(\Omega)$ be a simplicial triangulation obtained by refinement from $\mathcal{T}_H(\Omega)$. Then, for any $0 < \varepsilon_1 < 1$ and $v \in V + V_H$ it holds*

$$a_h^{IP}(v, v) \leq (1 + \varepsilon_1) a_H^{IP}(v, v) + \left(\frac{C_L}{\gamma \varepsilon_1} + 1 \right) \left(\eta_{h,C}^2 + \eta_{H,C}^2 \right). \quad (3.41)$$

Proof: For $v \in V + V_H$ we have

$$\begin{aligned} a_h^{IP}(v, v) &= \sum_{T \in \mathcal{T}_h(\Omega)} \|\nabla v\|_{0,T}^2 + \sum_{E \in \mathcal{E}_h(\Omega \cup \Gamma_D)} \frac{\alpha}{h_E} \|[v]_E\|_{0,E}^2 \\ &\quad - 2 \sum_{T \in \mathcal{T}_h(\Omega)} \left((\operatorname{Re}(L(v)), \operatorname{Re}(\nabla v))_{0,T} + (\operatorname{Im}(L(v)), \operatorname{Im}(\nabla v))_{0,T} \right). \end{aligned} \quad (3.42)$$

Obviously, the following relationships hold true

$$\sum_{T \in \mathcal{T}_h(\Omega)} |v|_{1,T}^2 = \sum_{T \in \mathcal{T}_H(\Omega)} |v|_{1,T}^2, \quad (3.43a)$$

$$\sum_{E \in \mathcal{E}_h(\Omega \cup \Gamma_D)} \frac{\alpha}{h_E} \|[v]_E\|_{0,E,h}^2 \leq 2 \sum_{E \in \mathcal{E}_H(\Omega \cup \Gamma_D)} \frac{\alpha}{H_E} \|[v]_E\|_{0,E,H}^2. \quad (3.43b)$$

3.4. QUASI-ORTHOGONALITY

Using (3.43a) in (3.42), we find

$$\begin{aligned}
 a_h^{IP}(v, v) &= a_H^{IP}(v, v) + \sum_{E \in \mathcal{E}_h(\Omega \cup \Gamma_D)} \frac{\alpha}{h_E} \|[v]_E\|_{0,E}^2 - \sum_{E \in \mathcal{E}_H(\Omega \cup \Gamma_D)} \frac{\alpha}{H_E} \|[v]_E\|_{0,E}^2 \quad (3.44) \\
 &- 2 \sum_{T \in \mathcal{T}_h(\Omega)} \left((\operatorname{Re}(L(v)), \operatorname{Re}(\nabla v))_{0,T} + (\operatorname{Im}(L(v)), \operatorname{Im}(\nabla v))_{0,T} \right) \\
 &+ 2 \sum_{T \in \mathcal{T}_H(\Omega)} \left((\operatorname{Re}(L(v)), \operatorname{Re}(\nabla v))_{0,T} + (\operatorname{Im}(L(v)), \operatorname{Im}(\nabla v))_{0,T} \right).
 \end{aligned}$$

The assertion follows by using Young's inequality in (3.44) and taking (3.10),(3.12a), and (3.43a),(3.43b) into account. \square

3.4.2 Lower order Term

The following result, which will be strongly needed in the derivation of the quasi-orthogonality result (cf. Theorem 3.4.1 below), is concerned with an estimate of the lower order term

$$2 k^2 \operatorname{Re}(c(u - u_h^c, u_h^c - u_H^c) + ikr(u - u_h^c, u_h^c - u_H^c))$$

where $u_h^c \in V_h^c, u_H^c \in V_H^c$ are the conforming approximations of (3.3). The proof uses the following regularity assumption:

(A) The solution u of (3.3) is $(1+r)$ -regular for some $r \in (1/2, 1]$, i.e., it satisfies $u \in V \cap H^{1+r}(\Omega)$ and for some positive constant C it holds

$$\|u\|_{1+r,\Omega} \leq C \left(\|f\|_{0,\Omega} + \|g\|_{0,\Gamma_R} \right). \quad (3.45)$$

3.4. QUASI-ORTHOGONALITY

Lemma 3.4.2 *Let $\mathcal{T}_h(\Omega)$ be a simplicial triangulation obtained by refinement from $\mathcal{T}_H(\Omega)$ and let $u_h^c \in V_h^c, u_H^c \in V_H^c$ be the conforming approximations of (3.3). Then, under assumption (A), there exists a constant $C_{LT} > 0$, depending on the local geometry of the triangulations, such that*

$$\begin{aligned} 2\operatorname{Re}(k^2 c(u - u_h^c, u_H^c - u_h^c) + ikr(u - u_h^c, u_H^c - u_h^c)) &\leq \\ C_{LT} h^r \left(|u - u_h^c|_{1,\Omega}^2 + |u_H^c - u_h^c|_{1,\Omega}^2 \right). \end{aligned} \quad (3.46)$$

Proof: Using a trace inequality, by straightforward estimation we deduce the existence of a constant $C_{L1} > 0$ such that

$$\begin{aligned} 2k^2 \operatorname{Re}(c(u - u_h^c, u_H^c - u_h^c) + ik r(u - u_h^c, u_H^c - u_h^c)) \\ \leq C_{L1} |u - u_h^c|_{1,\Omega} \left(\|u_H^c - u_h^c\|_{0,\Omega} + \|u_H^c - u_h^c\|_{0,\Gamma_R} \right). \end{aligned} \quad (3.47)$$

We define $z^c \in V$ as the solution of

$$a(v^c, z^c) - k^2 c(v^c, z^c) + ik r(v^c, z^c) \quad (3.48)$$

$$= (u_H^c - u_h^c, v^c)_{0,\Omega} + (u_H^c - u_h^c, v^c)_{0,\Gamma_R}, \quad v^c \in V. \quad (3.49)$$

Due to the regularity result (3.45), we have $z^c \in V \cap H^{1+r}(\Omega)$ and there exists a constant $C_R > 0$ depending on the domain Ω such that

$$\|z^c\|_{1+r,\Omega} \leq C_R \left(\|u_H^c - u_h^c\|_{0,\Omega} + \|u_H^c - u_h^c\|_{0,\Gamma_R} \right). \quad (3.50)$$

Choosing $v^c = u_H^c - u_h^c$ in (3.48) and observing Galerkin orthogonality, the trace inequality, the interpolation estimate

$$\|z^c - I_h z^c\|_{1,\Omega} \leq C_I h^r \|z^c\|_{1+r,\Omega}$$

3.4. QUASI-ORTHOGONALITY

and (3.50), we deduce the existence of a constant $C_{L2} > 0$, depending on C_I, C_R , and C_T such that

$$\begin{aligned}
 & 2^{-1} \left(\|u_H^c - u_h^c\|_{0,\Omega} + \|u_H^c - u_h^c\|_{0,\Gamma_R} \right)^2 \leq \|u_H^c - u_h^c\|_{0,\Omega}^2 + \|u_H^c - u_h^c\|_{0,\Gamma_R}^2 = \\
 & a(u_H^c - u_h^c, z^c) - k^2 c(u_H^c - u_h^c, z^c) + ik r(u_H^c - u_h^c, z^c) = \\
 & a(u_H^c - u_h^c, z^c - I_h z^c) - k^2 c(u_H^c - u_h^c, z^c - I_h z^c) + ik r(u_H^c - u_h^c, z^c - I_h z^c) \\
 & \leq C_{L2} h^r |u_H^c - u_h^c|_{1,\Omega} \left(\|u_H^c - u_h^c\|_{0,\Omega} + \|u_H^c - u_h^c\|_{0,\Gamma_R} \right),
 \end{aligned}$$

whence

$$\|u_H^c - u_h^c\|_{0,\Omega} + \|u_H^c - u_h^c\|_{0,\Gamma_R} \leq 2 C_{L2} h^r |u_H^c - u_h^c|_{1,\Omega}. \quad (3.51)$$

Hence, choosing $C_{LT} := 4C_{L1}C_{L2}$, the assertion follows from (3.47) and (3.51). \square

3.4.3 Quasi-orthogonality

In this subsection, we prove the following quasi-orthogonality result:

Theorem 3.4.1 *Let $\mathcal{T}_h(\Omega)$ be a simplicial triangulation obtained by refinement from $\mathcal{T}_H(\Omega)$, and let $u_h \in V_h$, $u_H \in V_H$ and η_h, η_H be the associated solutions of (3.7) and error estimators, respectively. Further, let $e_h := u - u_h$ and $e_H := u - u_H$ be the fine and coarse mesh errors. Then, for any $0 < \varepsilon < 1$ there exists a meshwidth $h_{max} > 0$, depending on the wavenumber k , the domain Ω and ε , and a constant*

3.4. QUASI-ORTHOGONALITY

$C_Q > 0$, depending on $\gamma, C_1, C_{ce}, C_{LT}$, and k , such that for all $h \leq h_{max}$ it holds

$$a_h^{IP}(e_h, e_h) \leq \tag{3.52}$$

$$(1 + \varepsilon) a_H^{IP}(e_H, e_H) - \frac{\gamma}{8} \|u_h - u_H\|_{1,h,\Omega}^2 + \frac{C_Q}{\alpha} (\eta_h^2 + \eta_H^2).$$

Proof: With $u_h^c \in S_h$ and $u_H^c \in S_H$ as the conforming P1 approximations of (3.3) with respect to the triangulations $\mathcal{T}_h(\Omega)$ and $\mathcal{T}_H(\Omega)$ we have

$$a_h^{IP}(e_h, e_h) = a_h^{IP}(e_h + u_h^c - u_H^c, e_h + u_h^c - u_H^c) \tag{3.53}$$

$$+ 2 \operatorname{Re} a_h^{IP}(e_h, u_H^c - u_h^c) - a_h^{IP}(u_h^c - u_H^c, u_h^c - u_H^c).$$

The three terms on the right-hand side in (3.53) will be estimated separately. These estimates will be provided by the following three lemmas.

Lemma 3.4.3 *Under the same assumptions as in Theorem 3.4.1 there exists a constant $C_2 > 0$, depending on γ, C_1, C_{ce}, C_J , and C_L , such that for any $0 < \hat{\varepsilon} < 1/2$ there holds*

$$a_h^{IP}(e_h + u_h^c - u_H^c, e_h + u_h^c - u_H^c) \leq (1 + \hat{\varepsilon}) a_H^{IP}(e_H, e_H) + \frac{C_2}{\alpha} (\eta_h^2 + \eta_H^2). \tag{3.54}$$

Proof: We split the first term on the right-hand side of (3.53) according to

$$a_h^{IP}(u - u_h + u_h^c - u_H^c, u - u_h + u_h^c - u_H^c) = \tag{3.55}$$

$$a_h^{IP}(e_H + u_H^{nc} - u_h^{nc}, e_H + u_H^{nc} - u_h^{nc}).$$

3.4. QUASI-ORTHOGONALITY

Using (3.12b), Young's inequality, and Corollary 3.3.2, we find

$$\begin{aligned}
 & a_h^{IP}(e_H + u_H^{nc} - u_h^{nc}, e_H + u_H^{nc} - u_h^{nc}) \\
 & \leq a_h^{IP}(e_H, e_H) + C_1 \|u_h^{nc} - u_H^{nc}\|_{1,h,\Omega}^2 + 2C_1^{1/2} a_h^{IP}(e_H, e_H)^{1/2} \|u_h^{nc} - u_H^{nc}\|_{1,h,\Omega} \\
 & \leq (1 + \varepsilon_2) a_h^{IP}(e_H, e_H) + C_1 \left(1 + \frac{1}{\varepsilon_2}\right) \|u_h^{nc} - u_H^{nc}\|_{1,h,\Omega}^2 \\
 & \leq (1 + \varepsilon_2) a_h^{IP}(e_H, e_H) + 4C_1 \frac{C_{ce}}{\alpha} \left(1 + \frac{1}{\varepsilon_2}\right) (\eta_h^2 + \eta_H^2).
 \end{aligned} \tag{3.56}$$

For the first term on the right-hand side in (3.56), the mesh perturbation result (3.41) and a subsequent application of (3.15) tell us

$$a_h^{IP}(e_H, e_H) \leq (1 + \varepsilon_1) a_H^{IP}(e_H, e_H) + \frac{2C_J C_L}{\alpha \varepsilon_1 \gamma^2} (\eta_h^2 + \eta_H^2). \tag{3.57}$$

Choosing $0 < \varepsilon_i < 1, 1 \leq i \leq 2$, such that $\hat{\varepsilon} := \varepsilon_1 + \varepsilon_2 + \varepsilon_1 \varepsilon_2 < 1/2$, and

$$C_2 := 2(1 + \varepsilon_2) \frac{C_J C_L}{\varepsilon_1 \gamma^2} + 4C_1 C_{ce} \left(1 + \frac{1}{\varepsilon_2}\right),$$

the assertion follows from (3.56) and (3.57). \square

Lemma 3.4.4 *Under the same assumptions as in Theorem 3.4.1, there exists a constant $C_i > 0, 3 \leq i \leq 6$, depending on γ, C_{ce} , and C_{LT} , such that*

$$\begin{aligned}
 & 2 \operatorname{Re} a_h^{IP}(e_h, u_H^c - u_h^c) \leq \\
 & C_3 h^r a_h^{IP}(e_h, e_h) + \left(\frac{\gamma}{4} + C_4 h^r\right) \|u_h - u_H\|_{1,h,\Omega}^2 + \frac{C_5 + C_6 h^r}{\alpha} (\eta_h^2 + \eta_H^2),
 \end{aligned} \tag{3.58}$$

where $C_3 := 2 C_{LT}/\gamma, C_4 := 3C_{LT}$, and the positive constants C_5, C_6 depend on the wavenumber k and on C_{ce}, C_{LT} .

3.4. QUASI-ORTHOGONALITY

Proof: For the second term on the right-hand side of (3.53) we have

$$\begin{aligned}
 2 \operatorname{Re}\left(a_h^{IP}(e_h, u_H^c - u_h^c)\right) &= 2 \operatorname{Re}\left(k^2 c(e_h, u_H^c - u_h^c) + ik r_h(e_h, u_H^c - u_h^c)\right) \\
 &= 2 \operatorname{Re}\left((k^2 c(u - u_h^c, u_H^c - u_h^c) + ik r(u - u_h^c, u_H^c - u_h^c))\right) + \\
 &\quad 2 \operatorname{Re}\left(k^2 c(u_h^c - u_h, u_H^c - u_h^c) + ik r(u_h^c - u_h, u_H^c - u_h^c)\right).
 \end{aligned} \tag{3.59}$$

In view of Lemma 3.4.2, the first term on the right-hand side in (3.59) can be estimated as follows

$$\begin{aligned}
 &2 \operatorname{Re}\left((k^2 c(u - u_h^c, u_H^c - u_h^c) + ik r(u - u_h^c, u_H^c - u_h^c))\right) \\
 &\leq C_{LT} h^r \left(|e_h^c|_{1,h,\Omega}^2 + |u_H^c - u_h^c|_{1,h,\Omega}^2\right).
 \end{aligned} \tag{3.60}$$

Taking advantage of (3.12a) and Corollary 3.3.2, for the two terms on the right-hand side in (3.60) we find

$$\begin{aligned}
 |e_h^c|_{1,h,\Omega}^2 &\leq 2 \left(\|u - u_h\|_{1,h,\Omega}^2 + \|u_h - u_h^c\|_{1,h,\Omega}^2\right) \\
 &\leq \frac{2}{\gamma} a_h^{IP}(e_h, e_h) + 2 \frac{C_{ce}}{\alpha} \eta_h^2, \\
 |u_H^c - u_h^c|_{1,h,\Omega}^2 &\leq 3 \left(\|u_H - u_h\|_{1,h,\Omega}^2 + \|u_H^c - u_H\|_{1,h,\Omega}^2 + \|u_h - u_h^c\|_{1,h,\Omega}^2\right) \\
 &\leq 3 \|u_H - u_h\|_{1,h,\Omega}^2 + 6 \frac{C_{ce}}{\alpha} \left(\eta_h^2 + \eta_H^2\right)
 \end{aligned}$$

and hence,

$$\begin{aligned}
 &2 \operatorname{Re}\left(k^2 c(u - u_h^c, u_H^c - u_h^c) + ik r(u - u_h^c, u_H^c - u_h^c)\right) \\
 &\leq \frac{2}{\gamma} C_{LT} h^r a_h^{IP}(e_h, e_h) + 3 C_{LT} h^r \|u_H - u_h\|_{1,h,\Omega}^2 + 8 \frac{C_{ce} C_{LT}}{\alpha} h^r \left(\eta_h^2 + \eta_H^2\right).
 \end{aligned} \tag{3.61}$$

3.4. QUASI-ORTHOGONALITY

We split the second term on the right-hand side in (3.59) according to

$$\begin{aligned}
 & 2 \operatorname{Re} \left(k^2 c_h(u_h^c - u_h, u_H^c - u_h^c) + ik r_h(u_h^c - u_h, u_H^c - u_h^c) \right) = \\
 & 2 \operatorname{Re} \left(k^2 c_h(u_h^c - u_h, u_H^c - u_H) + ik r_h(u_h^c - u_h, u_H^c - u_H) \right) + \\
 & 2 \operatorname{Re} \left(k^2 c_h(u_h^c - u_h, u_H - u_h) + ik r_h(u_h^c - u_h, u_H - u_h) \right) + \\
 & 2 \operatorname{Re} \left(k^2 c_h(u_h^c - u_h, u_h - u_h^c) + ik r_h(u_h^c - u_h, u_h - u_h^c) \right). \tag{3.62}
 \end{aligned}$$

By (3.31) and Young's inequality, the three terms on the right-hand side in (3.62) can be estimated as follows

$$\begin{aligned}
 & 2 \operatorname{Re} \left(k^2 c_h(u_h^c - u_h, u_H^c - u_H) + ik r_h(u_h^c - u_h, u_H^c - u_H) \right) \\
 & \leq 4 \max(k, k^2) \frac{C_{ce}}{\alpha} \eta_h^2, \\
 & 2 \operatorname{Re} \left(k^2 c_h(u_h^c - u_h, u_H - u_h) + ik r_h(u_h^c - u_h, u_H - u_h) \right) \\
 & \leq \frac{\gamma}{4} \|u_H - u_h\|_{1,h,\Omega}^2 + \frac{4C_{ce}}{\alpha\gamma} (\max(k, k^2))^2 \eta_h^2, \\
 & 2 \operatorname{Re} \left(k^2 c_h(u_h^c - u_h, u_h - u_h^c) + ik r_h(u_h^c - u_h, u_h - u_h^c) \right) \\
 & \leq 2 \frac{C_{ce}}{\alpha} \max(k, k^2) (\eta_h^2 + \eta_H^2).
 \end{aligned}$$

Then, (3.58) follows from (3.59)-(3.62) and the preceding estimates. \square

Lemma 3.4.5 *Under the same assumptions as in Theorem 3.4.1, there exists a constant $C_7 > 0$ such that*

$$a_h^{IP}(u_h^c - u_H^c, u_h^c - u_H^c) \geq \frac{\gamma}{2} \|u_h - u_H\|_{1,h,\Omega}^2 - \frac{C_7}{\alpha} (\eta_h^2 + \eta_H^2). \tag{3.63}$$

3.5. CONTRACTION PROPERTY

Proof: Taking into account (3.12a) and using Young's inequality and (3.31) we find

$$\begin{aligned}
 a_h^{IP}(u_h^c - u_H^c, u_h^c - u_H^c) &\geq \gamma \|u_h^c - u_H^c\|_{1,h,\Omega}^2 \geq \gamma \left(\|u_h - u_H\|_{1,h,\Omega}^2 + \right. & (3.64) \\
 &\left. \|u_h^c - u_h + u_H - u_H^c\|_{1,h,\Omega}^2 - 2|(u_h - u_H, u_h^c - u_h + u_H - u_H^c)_{1,h,\Omega}| \right) \\
 &\geq \left(\gamma - \frac{\varepsilon}{2}\right) \|u_h - u_H\|_{1,h,\Omega}^2 - 4\gamma \varepsilon^{-1} \left(\|u_h^{nc}\|_{1,h,\Omega}^2 + \|u_H^{nc}\|_{1,h,\Omega}^2 \right) \\
 &\geq \left(\gamma - \frac{\varepsilon}{2}\right) \|u_h - u_H\|_{1,h,\Omega}^2 - 4\gamma \frac{C_{ce}}{\alpha\varepsilon} \left(\eta_h^2 + \eta_H^2 \right).
 \end{aligned}$$

Then, (3.63) follows from (3.64) for $\varepsilon = \gamma$ with $C_7 := 4C_{ce}$. \square

Proof of Theorem 3.4.1. Using the estimates from Lemma 3.4.3, Lemma 3.4.4, and 3.4.5 in (3.53), we obtain

$$\begin{aligned}
 a_h^{IP}(e_h, e_h) &\leq \frac{1 + \hat{\varepsilon}}{1 - C_3 h^r} a_H^{IP}(e_H, e_H) - \frac{\gamma/4 - c_4 h^r}{1 - C_3 h^r} \|u_h - u_H\|_{1,h,\Omega}^2 & (3.65) \\
 &\quad + \frac{C_5 + C_6 h^r + C_7}{\alpha(1 - C_3 h^r)} \left(\eta_h^2 + \eta_H^2 \right).
 \end{aligned}$$

We choose $h_{max} > 0$ such that

$$\frac{1 + \hat{\varepsilon}}{1 - C_3 h_{max}^r} \leq 1 + 2\hat{\varepsilon}, \quad \frac{\gamma/4 - c_4 h_{max}^r}{1 - C_3 h_{max}^r} \geq \gamma/8. \quad (3.66)$$

Then, (3.52) follows from (3.65) with $\varepsilon := 2\hat{\varepsilon}$ and $C_Q := (C_5 + C_6 h_{max}^r + C_7)/(1 - C_3 h_{max}^r)$. \square

3.5 Contraction Property

We now use the monotonicity result (3.36) and the quasiorthogonality (3.52) to prove the following contraction property:

3.5. CONTRACTION PROPERTY

Theorem 3.5.1 *Let $u \in H_{0,\Gamma_D}^1(\Omega)$ be the unique solution of (3.3). Further, let $\mathcal{T}_h(\Omega)$ be a simplicial triangulation obtained by refinement from $\mathcal{T}_H(\Omega)$, and let $u_h \in V_h$, $u_H \in V_H$ and η_h, η_H be the associated solutions of (3.7) and error estimators, respectively. Then, there exist constants $0 < \delta < 1$ and $\rho > 0$, depending only on the shape regularity of the triangulations and the parameter θ from the Dörfler marking, such that for sufficiently large penalty parameter α and sufficiently small mesh widths h, H the fine mesh and coarse mesh discretization errors $e_h := u - u_h$ and $e_H = u - u_H$ satisfy*

$$a_h^{IP}(e_h, e_h) + \rho \eta_h^2 \leq \delta \left(a_H^{IP}(e_H, e_H) + \rho \eta_H^2 \right). \quad (3.67)$$

Proof: Multiplying the estimator reduction property (3.38) by $\gamma/(8C_\tau)$ and substituting the result into the quasi-orthogonality estimate (3.52), for $\rho > 0$ we get

$$\begin{aligned} a_h^{IP}(e_h, e_h) + \rho \eta_h^2 &\leq (1 + \varepsilon) a_H^{IP}(e_H, e_H) \\ &+ \left(\frac{C_Q}{\alpha} - \frac{\gamma}{8C_\tau} + \rho \right) \eta_h^2 + \left(\frac{C_Q}{\alpha} + \frac{\gamma\tau(\theta)}{8C_\tau} \right) \eta_H^2. \end{aligned} \quad (3.68)$$

For the choice

$$\alpha > \frac{8C_Q C_\tau}{\gamma}, \quad \rho := \frac{\gamma}{8C_\tau} - \frac{C_Q}{\alpha} \quad (3.69)$$

it follows from (3.68) that

$$a_h^{IP}(e_h, e_h) + \rho \eta_h^2 \leq (1 + \varepsilon) a_H^{IP}(e_H, e_H) + \left(\frac{C_Q}{\alpha} + \frac{\gamma\tau(\theta)}{8C_\tau} \right) \eta_H^2.$$

3.5. CONTRACTION PROPERTY

Invoking the reliability (3.39) of the estimator, we find

$$a_h^{IP}(e_h, e_h) + \rho \eta_h^2 \leq \quad (3.70)$$

$$\delta a_H^{IP}(e_H, e_H) + \left((1 + \varepsilon) - \delta \right) a_H^{IP}(e_H, e_H) + \frac{\gamma\tau(\theta)}{8C_\tau} \eta_H^2 \leq \quad (3.71)$$

$$\delta a_H^{IP}(e_H, e_H) + \left(C_{rel} \left((1 + \varepsilon) - \delta \right) + \frac{C_Q}{\alpha} + \frac{\gamma\tau(\theta)}{8C_\tau} \right) \eta_H^2.$$

We choose δ such that

$$\rho = \frac{\gamma}{8C_\tau} - \frac{C_Q}{\alpha} = \delta^{-1} \left(C_{rel} \left((1 + \varepsilon) - \delta \right) + \frac{C_Q}{\alpha} + \frac{\gamma\tau(\theta)}{8C_\tau} \right). \quad (3.72)$$

Solving for δ , we obtain

$$\delta = \frac{C_{rel} \left(1 + \varepsilon \right) + \frac{C_Q}{\alpha} + \frac{\gamma\tau(\theta)}{8C_\tau}}{\frac{\gamma}{8C_\tau} - \frac{C_Q}{\alpha} + C_{rel}}. \quad (3.73)$$

Now, we choose

$$\begin{aligned} \tau = \tau^* &:= \frac{1}{2} \frac{(1 - 2^{-1/2}) \theta}{1 - (1 - 2^{-1/2}) \theta} < \frac{1}{4}, \\ \varepsilon &:= \frac{1}{2} \frac{\gamma (1 - \tau^*)}{8C_{rel}C_{\tau^*}} < 1. \end{aligned}$$

It follows that

$$\delta = \frac{C_{rel} + \frac{\gamma(1+\tau^*)}{16C_{\tau^*}} + \frac{C_Q}{\alpha}}{C_{rel} + \frac{\gamma}{8C_{\tau^*}} - \frac{C_Q}{\alpha}} \quad (3.74)$$

Looking for α such that

$$\frac{\gamma(1 + \tau^*)}{16C_{\tau^*}} + \frac{C_Q}{\alpha} < \frac{\gamma}{8C_{\tau^*}} - \frac{C_Q}{\alpha},$$

we find that $0 < \delta < 1$ for

$$\alpha > \frac{32C_Q C_{\tau^*}}{(1 - \tau^*)\gamma}. \quad (3.75)$$

This concludes the proof of the contraction property. \square

CHAPTER 4

Numerical Results

4.1 Introduction

This chapter is devoted to a documentation of numerical results that illustrate the performance of the adaptive IPDG method over a wide range of wavenumbers.

We begin with results of some initial numerical tests which were conducted for different polynomial orders of approximations and for wavenumbers $\kappa = 5, 10, 20$. Intuitively, these results provided some guidance towards an underlying dependence of the wavenumber and the polynomial order N . Next, we present four model problems for the Helmholtz equation with wavenumbers ranging from $\kappa = 5$ to $\kappa = 70$ using

polynomials of order upto order 6. In particular, the main application is the screen problem in two dimensions which describes the propagation of an acoustic wave and its scattering around a soft sound screen. For this problem we had no prior knowledge of the analytic solution. As expected, the residual-type error estimator detects the singularities and refines in precisely around the singularities.

These model problems demonstrate quasi-optimality which is in accordance with the theoretical results for the second-order elliptic boundary value problems (cf. [34]). Moreover, as can be expected, for a high wavenumber the asymptotic regime is reached later, i.e., for finer meshes, compared to lower wavenumbers. For all our numerical experiments we maintained consistent choice of the penalty parameter $\alpha = 50(N + 1)^2$ where N is the polynomial order.

4.2 Preliminary Results for Smooth Problems

Our preliminary numerical experiments were for the symmetric IPDG method tested on a smooth problem $u(x, y) = -\exp^{-i\kappa(x+y)}$ on the computational domain $\Omega = [-1, 1] \times [-1, 1]$, respecting the mesh constraint $\kappa h \lesssim 1$.

A clear dependence on the polynomial order for resolving higher wave numbers motivated us to investigate the impact of higher polynomial order on the convergence.

4.3. TEST PROBLEMS ON NON-CONVEX DOMAIN

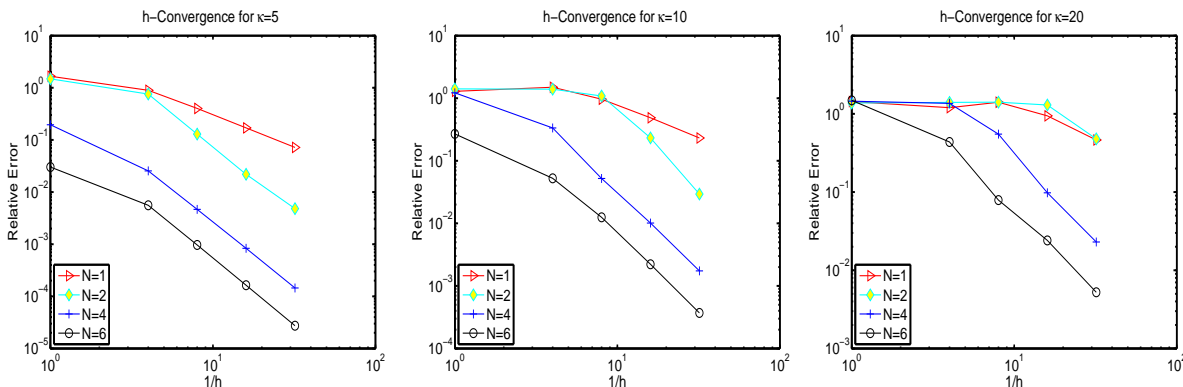


Figure 4.1: A comparison of the convergence for different polynomial order N for wave numbers $k = 5$ (left), $k = 10$ (center) and $k = 20$ (right) .

4.3 Test Problems on Non-convex Domain

In order to illustrate the convergence history of the adaptive IPDG approach in terms of the exact discretization error $e_h := u - u_h$ in the mesh dependent energy norm $a_h^{IP}(e_h, e_h)^{1/2}$, as a first example we choose an interior Dirichlet problem for the Helmholtz equation where the exact solution is known. In particular, we consider (3.1a) in a bounded polygonal domain $\Omega \subset \mathbb{R}^2$ with the boundary conditions (3.1b),(3.1c) replaced by a Dirichlet boundary condition on $\Gamma := \partial\Omega$.

$$\begin{aligned}
 -\Delta u - k^2 u &= f \quad \text{in } \Omega, \\
 u &= g \quad \text{on } \Gamma.
 \end{aligned}$$

We note that the preceding convergence analysis applies to such interior Dirichlet problems as well. Its implementation requires the appropriate changes made to the right hand side of the IPDG formulation (3.7).

Example 1: Consider the interior Dirichlet problem

$$-\Delta u - k^2 u = f \quad \text{in } \Omega, \tag{4.1a}$$

$$u = g \quad \text{on } \Gamma. \tag{4.1b}$$

The source terms f, g are chosen such that $u(r, \varphi) = J_{1/2}(kr)$ (in polar coordinates) is the exact solution, where $J_{1/2}(\cdot)$ stands for the Bessel function of the first kind. The solution is an oscillating function with decreasing amplitude for increasing r which exhibits a singularity at the origin (cf. Fig. 4.2 (left)). We tested this problem on two non-convex domains namely the notorious L-shaped domain (cf. 4.3.1) and the circular domain with a cut-out wedge (Pacman Problem) (cf. 4.3.2).

4.3.1 L-shaped Domain

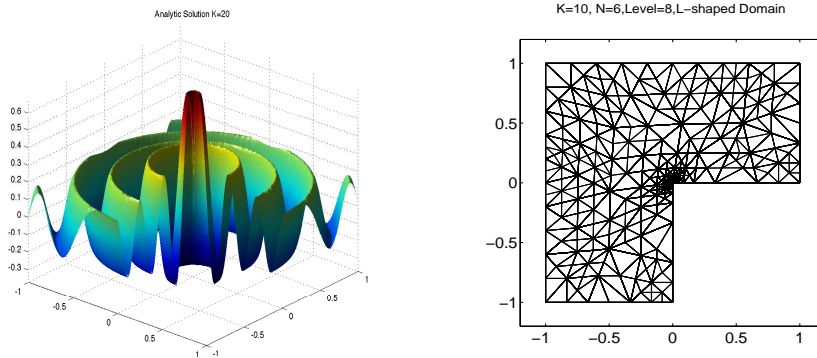


Figure 4.2: Exact solution for $k = 20$ (left) and adaptively refined grid after 8 refinement steps for $k = 10$, $N = 6$, and $\theta = 0.3$ (right).

We have applied the adaptive IPDG method to (4.1a),(4.1b) with $\Omega := (-1, +1)^2 \setminus [0, +1) \cup (-1, 0]$. For $k = 10$, $N = 6$, and $\theta = 0.3$, Figure 4.2 (right) shows the adaptively refined mesh after 8 refinement steps with a pronounced refinement in a vicinity of the singularity at the origin.

Figure 4.3 reflects the convergence history of the adaptive process. The mesh dependent energy norm $\|u - u_h\|_a := a_h^{IP}(u - u_h, u - u_h)^{1/2}$ of the error is displayed as a function of the total number of degrees of freedom on a logarithmic scale. The curves represent the decrease in the error both for uniform refinement and for adaptive refinement in case of different values of the constant θ in the Dörfler marking. In particular, Figure 4.3 (left) refers to the wavenumber $k = 5$ and the polynomial degree $N = 6$, whereas Figure 4.3 (right) shows the results for the wavenumber $k = 10$ and the same polynomial degree $N = 6$.

4.3. TEST PROBLEMS ON NON-CONVEX DOMAIN

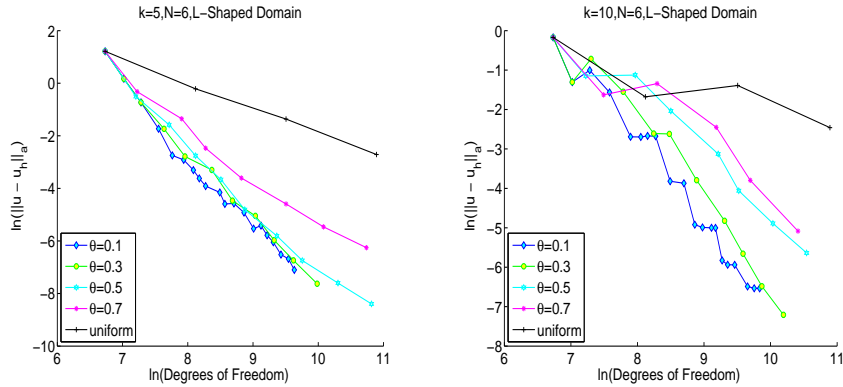


Figure 4.3: Convergence history of the adaptive IPDG method. Mesh dependent energy error as a function of the DOF (degrees of freedom) on a logarithmic scale: $k = 5$, $N = 6$ (left) and $k = 10$, $N = 6$ (left).

4.3.2 Pacman Problem

In this method curvilinear elements instead of straight sided elements are used to resolve the geometry of the domain. The geometrical representation by curvilinear elements complements the performance of the estimator as is evident from the refinement of the domain.

Figure 4.4 depicts the meshes obtained after 6 levels and 3 levels of the adaptive algorithm. Whereas, Figure 4.5, shows the plots of the convergence which is slower as compared to our previous example and this can be attributed to the curved nature of the domain.

4.3. TEST PROBLEMS ON NON-CONVEX DOMAIN

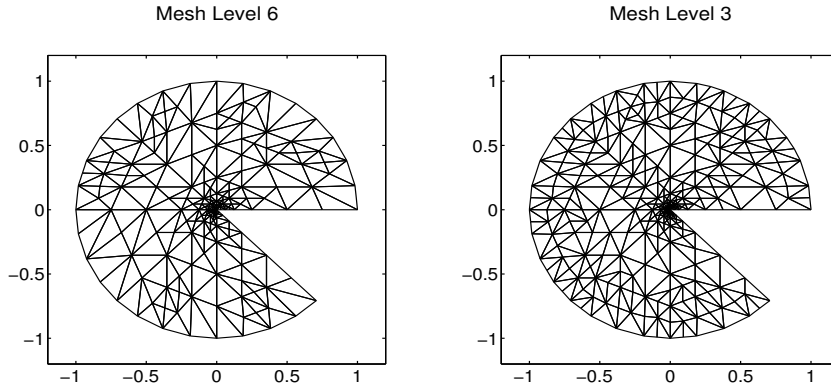


Figure 4.4: Adaptively refined grids for $k = 1$, $N = 4$, $\theta = 0.1$ (left) and $k = 5$, $N = 6$, $\theta = 0.3$ (right) after 6 and 3 levels of the adaptive cycle .

4.3.3 Screen Problem

The next example deals with the screen problem (3.1a)-(3.1c).

Example 2: We choose $\Omega := (-1, +1)^2 \setminus (S_1 \cup S_2)$ where

$$S_1 := \text{conv}((0, 0), (-0.25, +0.50), (-0.50, +0.50)),$$

$$S_2 := \text{conv}((0, 0), (+0.25, -0.50), (+0.50, -0.50)),$$

such that $\Gamma_R = \partial(-1, +1)^2$ and $\Gamma_D := \partial S_1 \cup \partial S_2$. The right-hand sides f and g are chosen according to $f \equiv 0$ and

$$g = \cos(kx_2) + i\sin(kx_2).$$

The real part of the computed IPDG approximation is shown in Figure 4.4 for wavenumber $k = 15$ (left) and for wavenumber $k = 20$ (right).

Figure 4.7 contains the adaptively refined mesh for wavenumber $k = 10$ and

4.3. TEST PROBLEMS ON NON-CONVEX DOMAIN

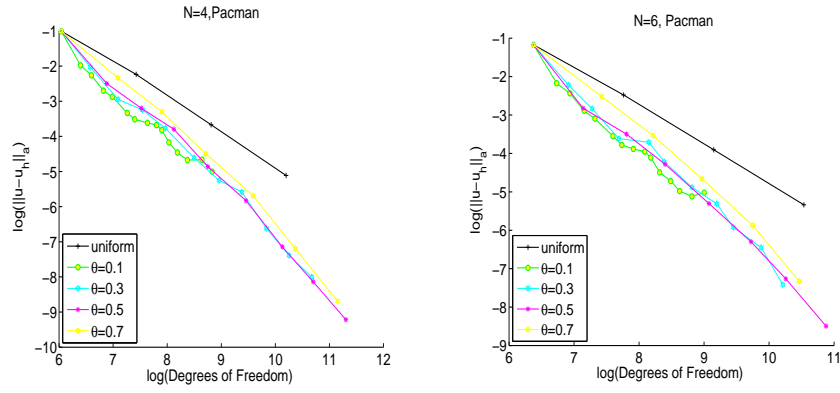


Figure 4.5: Convergence history of the adaptive IPDG method. Mesh dependent energy error as a function of the DOF (degrees of freedom) on a logarithmic scale: $k = 5$, $N = 4$ (left) and $k = 5$, $N = 6$ (left).

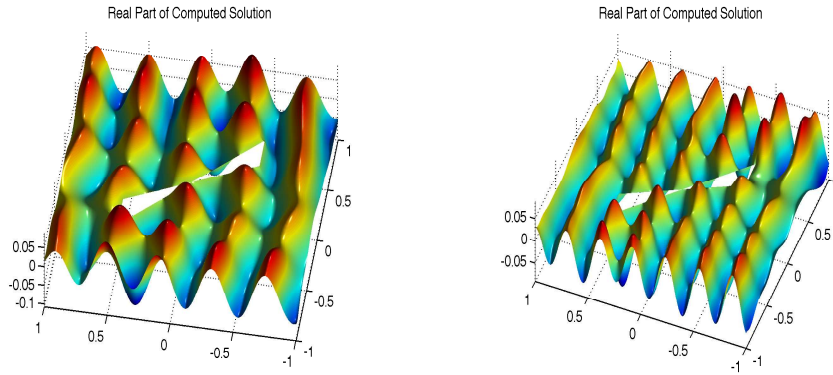


Figure 4.6: Real part of the computed IPDG approximation for $k = 15$ (left) and $k = 20$ (right).

4.3. TEST PROBLEMS ON NON-CONVEX DOMAIN

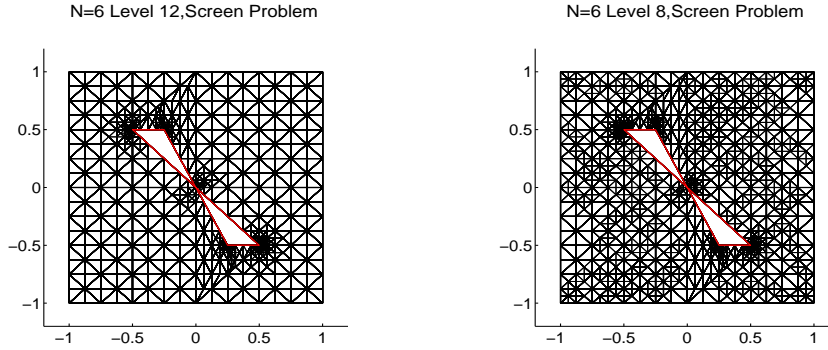


Figure 4.7: Adaptively refined mesh for $k = 10$, $N = 6$ after 8 refinement steps (left) and for $k = 20$, $N = 6$ after 12 refinement steps (right).

polynomial degree $N = 6$ after 12 refinement steps (left) and for wavenumber $k = 20$ and polynomial degree $N = 6$ after 8 refinement steps (right).

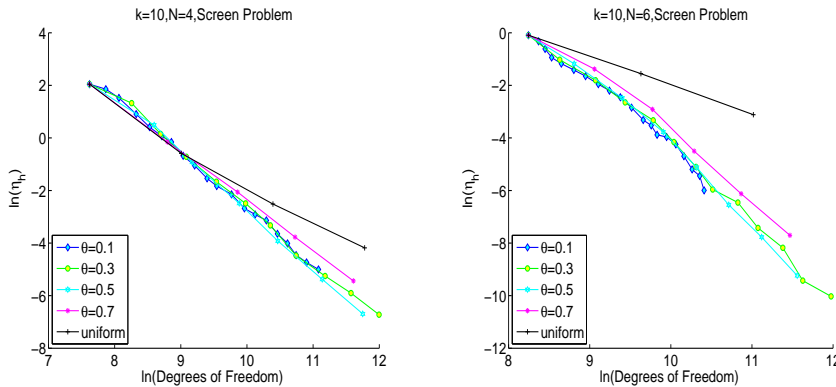


Figure 4.8: Convergence history of the adaptive IPDG method. Error estimator as a function of the DOF (degrees of freedom) on a logarithmic scale: $k = 10$, $N = 4$ (left) and $k = 10$, $N = 6$ (right).

Since we do not have access to the exact solution of the screen problem, we document the convergence history of the adaptive IPDG method by representing the decrease in the error estimator η_h as a function of the total number of degrees

4.3. TEST PROBLEMS ON NON-CONVEX DOMAIN

of freedom on a logarithmic scale. In particular, Figure 4.8 shows the results for wavenumber $k = 10$ and polynomial degree $N = 4$ (left) respectively polynomial degree $N = 6$ (right).

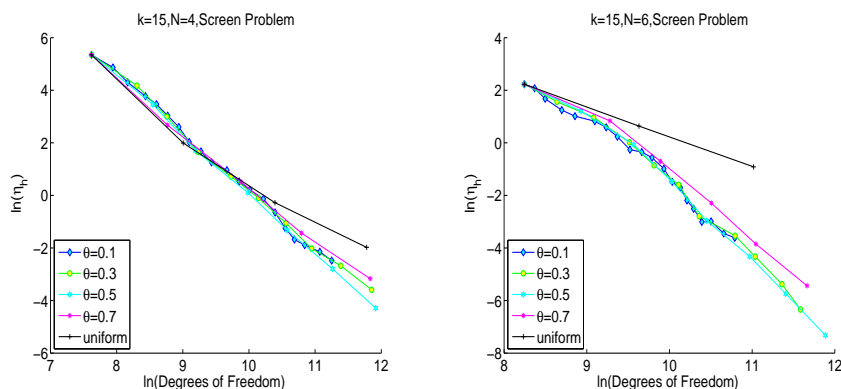


Figure 4.9: Convergence history of the adaptive IPDG method. Error estimator as a function of the DOF (degrees of freedom) on a logarithmic scale: $k = 15$, $N = 4$ (left) and $k = 15$, $N = 6$ (left).

Likewise, Figure 4.9 displays the convergence history for wavenumber $k = 15$ and polynomial degrees $N = 4$ (left) and $N = 6$ (right). We observe a similar behavior as in case of the interior Dirichlet problem in Section 4.3. For higher wavenumbers, the asymptotic regimes require fines meshes. Moreover, as we expect, higher polynomial degrees can handle higher wavenumbers better at the expense of increased computational work.

4.4 Convex Domain

Lastly, we consider the interior Dirichlet Problem on the convex computational domain $\Omega = (0, 1) \times (0, 1)$.

The source terms f, g are chosen such that $u(r, \varphi) = J_{\frac{3}{2}}(kr) \cos(\frac{3}{2}\theta)$ (in polar coordinates) is the exact solution. This solution is known to live in $H^{3/2+1-\varepsilon}(\Omega)$ for any $\varepsilon > 0$, but not in $H^{3/2+1}(\Omega)$ [Grisvard, [31] Theorem 1.4.5.3], with a corner singularity at the origin.

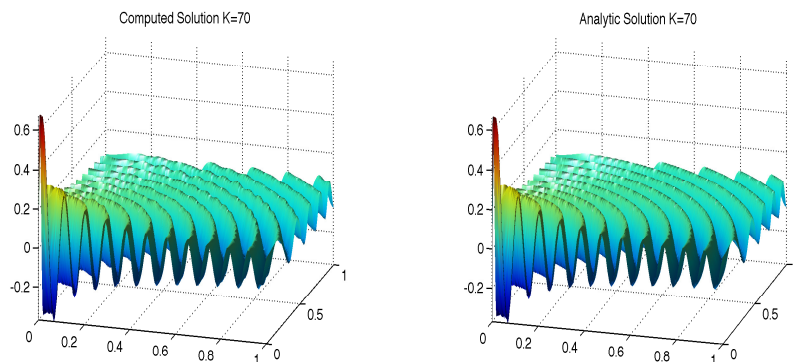


Figure 4.10: Computed solution (left) and exact solution (right) for $k = 70$.

The numerical solution of this problem by DG methods has been studied in [33] and [30]. In particular, the approach in [33] relies on a plane wave DG scheme, whereas in [30] a hybridized LDG method is used.

For the same choice of wavenumber $k = 4$ and with the use of the linear and quadratic elements, we observe the following h -convergence for our approach. In contrast to the results obtained by Griesmaier and Monk [Figure 2, page 12 in [30]

4.4. CONVEX DOMAIN

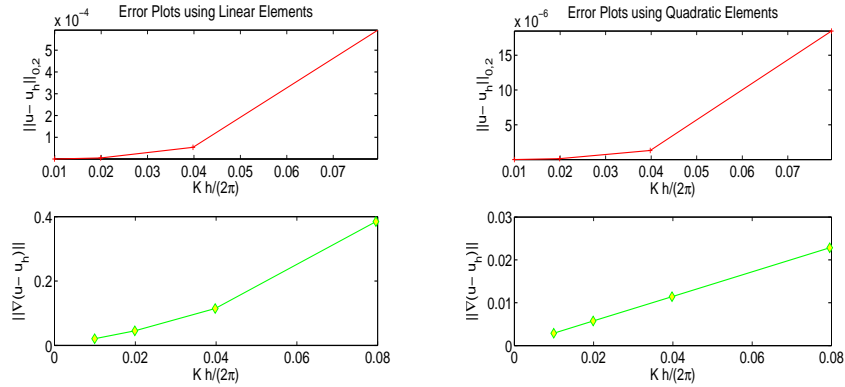


Figure 4.11: h -convergence using linear elements (left);quadratic elements (right).

], we notice a faster order of convergence for a coarser mesh size.

We report the convergence history of the error with respect to the mesh dependent energy norm (as shown in Figure 4.13)and with respect to L^2 - norm $\|u - u_h\|_{0,\Omega}$ (as shown in Figure 4.11) in relation to the total degrees of freedom.

In Figure 4.13, the accelerated decay of the error can be attributed to the improved regularity of our numerical solution.We also observe the impact of higher polynomial order approximation especially (as we mentioned in our introductory remarks) for large wavenumber this is evident from the significant change in the optimal order convergence.

4.4. CONVEX DOMAIN

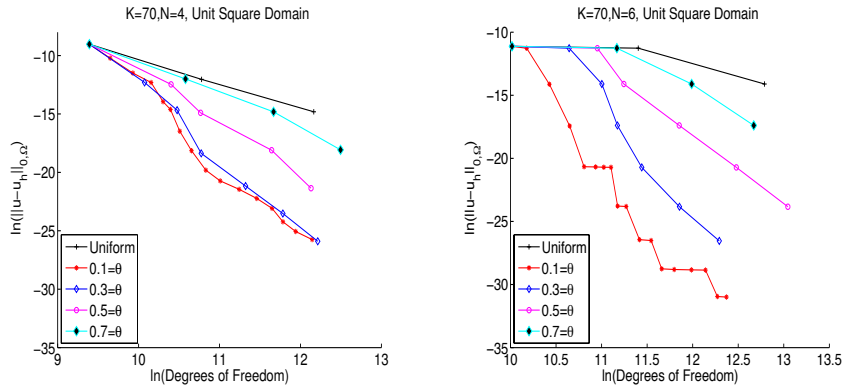


Figure 4.12: Convergence of the discretization error $\|u - u_h\|_{0,\Omega}$ as a function of the DOF (degrees of freedom) on a logarithmic scale: $k = 70$, $N = 4$ (left) and $k = 70$, $N = 6$ (left).

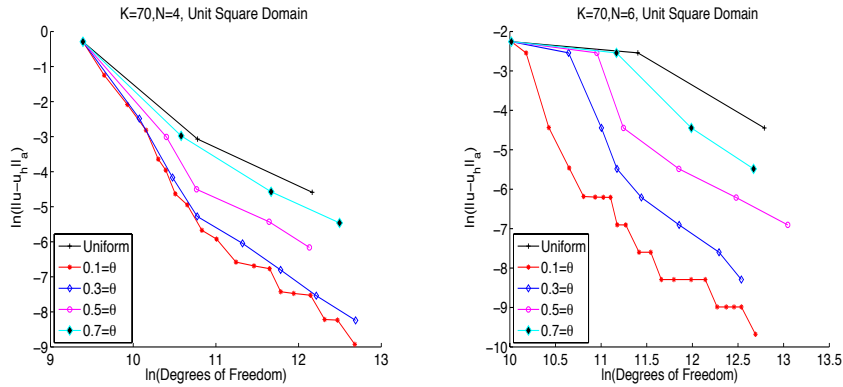


Figure 4.13: Convergence history of the adaptive IPDG method. Mesh dependent energy error as a function of the DOF (degrees of freedom) on a logarithmic scale: $k = 70$, $N = 4$ (left) and $k = 70$, $N = 6$ (left).

CHAPTER 6

Conclusions and Future Work

We have developed an adaptive symmetric Interior Penalty Discontinuous Galerkin (IPDG) method for the Helmholtz equation and analyzed its convergence by proving a contraction property for a weighted sum of the global discretization error in the IPDG energy norm and the residual-type a posteriori error estimator. The novelty in the convergence analysis compared to IPDG applied to standard second order elliptic boundary value problems is the appropriate treatment of the lower order term in the equation by resorting to the associated conforming approximation of the problem and using an Aubin-Nitsche type argument. We have illustrated the benefits of the adaptive IPDG approach by various numerical experiments which also revealed

quasi-optimality, although this property was not part of the theoretical convergence analysis.

An issue that remains to be addressed in future work is the development of an efficient and robust iterative solver for the IPDG discretized problem taking into account that the condition number significantly grows with increasing polynomial degree. The same issue can be expected for the hybridized version of the IPDG method which is computationally attractive due to the substantial reduction in the total number of degrees of freedom.

Finally, a natural extension of the present work would be to consider a similar IPDG method for interior domain problems associated with the time harmonic Maxwell equations, in particular, in the three-dimensional space. We believe that the convergence analysis essentially carries over with a somewhat more subtle Aubin-Nitsche type argument, but the solver issue will be even more challenging than for the Helmholtz equation due to the non-trivial kernel of the curl operator.

Bibliography

- [1] D.N. Arnold, F. Brezzi, B. Cockburn, and L.D. Marini, Unified analysis of discontinuous Galerkin methods for elliptic problems, *SIAM J. Numer. Anal.*, **39**, 1749-1779, 2002.
- [2] M. Ainsworth, A posteriori error estimation for Discontinuous Galerkin finite element approximation. *SIAM J. Numer. Anal.* **45**, 1777–1798, 2007.
- [3] M. Amara, R. Djellouli, and C. Farhat, Convergence analysis of a discontinuous Galerkin method with plane waves and lagrange multipliers for the solution of Helmholtz problems, *SIAM J. Numer. Anal.* **47**, 1038-1066, 2009.
- [4] G. B. Alvarez, A. F. D. Loula, E. G. Dutra do Carmo, and F. A. Rochinha, A discontinuous finite element formulation for Helmholtz equation. *Comput. Methods Appl. Mech. Engrg.* **195**, 4018-4035, 2006.
- [5] A. K. Aziz and A. Werschulz, On the numerical solutions of Helmholtz’s equation by the finite element method. *SIAM J. Numer. Anal.* **17**, 681-686, 1980.
- [6] I. Babuška, W.C. Rheinboldt, A posteriori error estimates for the finite element method. *International Journal for Numerical Methods in Engineering*, **12**, 1597-1615, 1978.
- [7] I. Babuška, W.C. Rheinboldt, Adaptive approaches and reliability estimates in finite element analysis. *Computer Methods in Applied Mechanics and Engineering*, **17-18**, Part 3, 519-540, 1979.

-
- [8] I. Babuška and S. Sauter, Is the pollution effect of the FEM avoidable for the Helmholtz equation?. *SIAM Review* **42**, 451-484, 2000.
- [9] I. Babuška and T. Strouboulis, *The Finite Element Method and its Reliability*. Clarendon Press, Oxford, 2001.
- [10] I. Babuška, T. Strouboulis, C. S. Upadhyay, and S. K. Gangaraj, A posteriori estimation and adaptive control of the pollution error in the h-version of the finite element method. *International Journal for Numerical Methods in Engineering*, **38**, 4207-4235, 1995.
- [11] Ihlenburg F, Babuška I. Finite element solution of the Helmholtz equation with high wavenumber part II: the h-p-version of the FEM. *SIAM Journal on Numerical Analysis*, **34**, 315 -358, 1997.
- [12] I. Babuška and W.C. Rheinboldt, Error estimates for adaptive finite element computations. *Siam J. Numer. Anal.*, **15**, 736-754, 1978.
- [13] W. Bangerth and R. Rannacher, *Adaptive Finite Element Methods for Differential Equations. Lectures in Mathematics. ETH-Zürich. Birkhäuser, Basel*, 2003.
- [14] R. Becker, P. Hansbo, and M.G. Larson, Energy norm a posteriori error estimation for discontinuous Galerkin methods. *Comput. Methods Appl. Mech. Engrg.* **192**, 723-733, 2003.
- [15] A. Bonito and R. Nochetto, Quasi-optimal convergence rate of an adaptive Discontinuous Galerkin method. *SIAM J. Numer. Anal.* **48**, 734-771, 2010.
- [16] C. Carstensen, T. Gudi, and M. Jensen, A unifying theory of a posteriori error control for discontinuous Galerkin FEM. *Numer. Math.* **112**, 363-379, 2009.
- [17] J.M. Cascon, Ch. Kreuzer, R.H. Nochetto, and K.G. Siebert, Quasi-optimal rate of convergence of adaptive finite element methods. *SIAM J. Numer. Anal.* **46**, 2524-2550, 2008.
- [18] C. L. Chang, A least-squares finite element method for the Helmholtz equation. *Comput. Methods Appl. Mech. Engrg.* **83**, 1-7, 1990.
- [19] L. Chen. Short bisection implementation in MATLAB. report, 2006.
- [20] E. T. Chung and B. Engquist, Optimal discontinuous Galerkin methods for wave propagation. *SIAM J. Numer. Anal.* **44**, 2131-2158, 2006.

-
- [21] B. Cockburn, Discontinuous Galerkin methods. *Z. Angew. Math. Mech.* **83**, 731–754, 2003.
- [22] D. Colton and P. Monk, The numerical solution of the three-dimensional inverse scattering problem for time harmonic acoustic waves. *SIAM J. Sci. Statist. Comput.* **8**, 278-291, 1987.
- [23] Dörfler, W.; A convergent adaptive algorithm for Poisson’s equation. *SIAM J. Numer. Anal.* **33**, 1106–1124, 1996.
- [24] B. Engquist and O. Runborg, Computational high frequency wave propagation. *Acta Numer.* **12**, 181-266, 2003.
- [25] X. Feng and H. Wu, Discontinuous Galerkin methods for the Helmholtz equation with large wave numbers. *SIAM J. Numer. Anal.* **47**, 2872-2896, 2009.
- [26] X. Feng and H. Wu, hp-discontinuous Galerkin methods for the Helmholtz equation with large wave number. submitted, arXiv:0907.3442v1, 2009.
- [27] G. Gabard, Discontinuous Galerkin methods with plane waves for time-harmonic problems. *J. Comp. Phys.* **225**, 1961-1984, 2007.
- [28] C. Gittelsohn, R. Hiptmair, and I. Perugia, Plane wave discontinuous Galerkin methods: Analysis of the h-version. *ESAIM: M2AN Math. Model. Numer. Anal.* **43**, 297-331, 2009.
- [29] J. Gopalakrishnan and J. Pasciak, Overlapping Schwarz preconditioners for indefinite time harmonic Maxwell equations. *Math. Comp.* **72**, 1–15, 2003.
- [30] R. Griesmaier and P. Monk, Error analysis for a hybridizable discontinuous Galerkin method for the Helmholtz equation. *J. Sci. Comp.* (in press), 2011.
- [31] P. Grisvard, *Elliptic Problems in Nonsmooth Domains*, Monographs and Studies in Mathematics, vol. 24, Pitman, Boston, MA, 1985.
- [32] J.S. Hesthaven and T. Warburton, *Nodal Discontinuous Galerkin Methods*. Springer, Berlin-Heidelberg-New York, 2008.
- [33] R. Hiptmair, A. Moiola, and I. Perugia, Plane wave Discontinuous Galerkin methods for the 2D Helmholtz equation: Analysis of the p-version, Report 2009-20, SAM, ETH Zürich, Zürich, Switzerland. Submitted to SINUM, 2009.
- [34] R.H.W. Hoppe, G. Kanschat, and T. Warburton, Convergence analysis of an adaptive interior penalty discontinuous Galerkin method. *SIAM J. Numer. Anal.*, **47**, 534–550, 2009.

- [35] P. Houston, D. Schötzau, and T.P. Wihler, Energy norm a posteriori error estimation of hp-adaptive discontinuous Galerkin methods for elliptic problems. *Math. Models Methods Appl. Sci.* **17**, 33–62, 2007.
- [36] F. Ihlenburg, *Finite Element Analysis of Acoustic Scattering*. Springer, Berlin-Heidelberg-New York, 1998.
- [37] F. Ihlenburg and I. Babuška, Finite element solution of the Helmholtz equation with high wave number. II. The h-p version of the FEM. *SIAM J. Numer. Anal.* **34**, 315–358, 1997.
- [38] N. A. Kampanis, J. Ekaterinaris, and V. Dougalis, *Effective Computational Methods for Wave Propagation*. Chapman & Hall/CRC, Boca Raton, 2008.
- [39] P. Monk and D. Wang, A least squares method for the Helmholtz equation, *Computer Methods in Applied Mechanics and Engineering* **175**. 121–136, 1999.
- [40] O. Karakashian and F. Pascal, A posteriori error estimates for a Discontinuous Galerkin approximation of second-order elliptic problems. *SIAM J. Numer. Anal.* **41**, 2374–2399, 2003.
- [41] O. Karakashian and F. Pascal, Convergence of adaptive Discontinuous Galerkin approximations of second-order elliptic problems. *SIAM J. Numer. Anal.* **45**, 641–665, 2007.
- [42] J.-C. Nédélec, *Acoustic and Electromagnetic Equations. Integral Representations for Harmonic Problems*, Springer, Berlin-Heidelberg-New York, 2001.
- [43] I. Perugia and D. Schötzau. An hp-analysis of the local discontinuous Galerkin method for diffusion problems. In *Proceedings of the Fifth International Conference on Spectral and High Order Methods (ICOSAHOM-01) (Uppsala)*, volume 17, pages 561–571, 2002.
- [44] B. Rivière, *Discontinuous Galerkin Methods for Solving Elliptic and Parabolic Equations. Theory and Implementation*. SIAM, Philadelphia, 2008.
- [45] B. Rivière and M.F. Wheeler, A posteriori error estimates and mesh adaptation strategy for discontinuous Galerkin methods applied to diffusion problems. *Computers & Mathematics with Applications* **46**, 141–163, 2003.
- [46] A. Schmidt and K. G. Siebert, *Design of Adaptive Finite Element Software: The Finite Element Toolbox ALBERTA*. Springer, Berlin-Heidelberg-New York, 2005.

- [47] D. Schötzau, C. Schwab, and A. Toselli, Mixed hp-dgfem for incompressible flows. *SIAM J. Numer. Anal.*, **40**, 2171–2194, 2003.
- [48] L. Tartar, *Introduction to Sobolev Spaces and Interpolation Theory*. Springer, Berlin-Heidelberg-New York, 2007.
- [49] L. Zhong, L. Chen, S. Shu, G. Wittum, and J. Xu, Convergence and optimality of adaptive edge finite element methods for time-harmonic Maxwell equations. Preprint, Department of Mathematics, University of California at Irvine, 2010.